

# Integration: An Effective Strategy to Develop Multifunctional Energy Storage Devices

Shaowu Pan, Jing Ren, Xin Fang, and Huisheng Peng\*

Energy storage devices are arousing increasing interest due to their key role in next-generation electronics. Integration is widely explored as a general and effective strategy aiming at high performances. Recent progress in integrating a variety of functions into electrochemical energy storage devices is carefully described. Through integration at the level of materials: flexible, stretchable, responsive, and self-healing devices are discussed to highlight the state-of-the-art multi-functional electronics. Through the integration at the level of devices, the incorporation of photovoltaic and piezoelectric devices is detailed to reflect the advances in self-powering electronics. Integrated energy storage devices are presented for wearable applications to indicate a new growth direction. The main challenges and important directions are summarized to offer some useful clues for future development.

LIBs generally meet the requirement of high energy density, while SCs are typically used for high power density based on the different working mechanisms. Some efforts are also made to achieve both high energy density and high power density by synthesizing functional materials and designing novel structures.<sup>[5–18]</sup> These advancements have been summarized in the other reviews and will not be covered here. However, the traditional LIBs and SCs that appear in a rigid bulky or planar structure cannot satisfy next-generation electronic devices. For instance, it is difficult for them to meet the requirements of being small, lightweight, flexible, weavable, adaptable, and self-powering from

## 1. Introduction

The increasing demand for high-performance portable electronic devices has stimulated rapid development in making them thin, lightweight, flexible, wearable and intelligent.<sup>[1–4]</sup> The concept for these advanced devices has been proposed for decades and often appears in various science fiction movies where they can be used in a variety of fields such as wearable electronic products, roll-up displays, implantable medical devices and sensors. Recently, some prototyped products have been also released from the sports field by Nike, Fitbit and Jawbone, to smart watches by Pebble, Garmin, Withings, LG and Apple, smart glasses by Google and smart clothes by AiQ and SunSang Fingers. This new technology represents a breakthrough in electronics and produced an explosion in the worldwide market. The number of these electronic devices will reach 126.1 million in 2019 according to the forecast data from the International Data Corporation.

Lithium ion batteries (LIBs) and supercapacitors (SCs) have been widely used as two main electrochemical energy storage devices, and play a key role in powering portable electronics.

wearable electronic devices.

Therefore, besides the continuous efforts to increase the energy storage capability, considerable interest has also been attracted to introducing smart components into conventional materials, and designing new structures aimed at more functions.<sup>[19–27]</sup> On one hand, flexible, stretchable, transparent, responsive, and self-healing properties are integrated into LIBs and SCs, in addition to storing energy, on the basis of the use of functional materials. On the other hand, the LIBs and SCs have been also integrated with various energy harvesting devices to realize the desired self-powering capability. To better achieve the practical application of the above energy storage devices, miniaturized structural design such as fiber-shaped LIBs and SCs has boomed over just a few years, and more attention is being paid to weaving them into powering fabrics.

Here, recent progress in developing high-performance energy storage devices by an integration strategy is highlighted to satisfy the next-generation electronics. Integration with more functions based on advanced materials is first discussed for multifunctional devices. Integration with energy harvesting devices is then provided for self-powering devices. The integration of LIBs and SCs into smart fabrics is followed to reflect a new booming direction in the energy storage industry. The current challenges and developing directions are finally summarized for future study.

Dr. S. Pan, J. Ren, X. Fang, Prof. H. Peng  
State Key Laboratory of Molecular  
Engineering of Polymers  
Department of Macromolecular Science  
and Laboratory of Advanced Materials  
Fudan University  
Shanghai 200438, China  
E-mail: penghs@fudan.edu.cn



DOI: 10.1002/aenm.201501867

## 2. Integration at the Level of Materials

High energy and power densities have been extensively explored since the discovery of LIBs and SCs, while the incorporation of more functions has become increasingly important, particularly

in recent years. The main functions, including being flexible, stretchable, transparent, responsive, and self-healing are carefully discussed in the following sections to reflect the key advancements in this field.

## 2.1. Flexible Materials

To achieve a flexible LIB or SC, it is required for the electrode, electrolyte, and packing materials to all be flexible.<sup>[28–33]</sup> As the flexible packing materials are commercially available, the main efforts are made to develop flexible electrodes and electrolytes with high electrochemical performances. The preparation of electrodes for a conventional LIB is mainly based on a slurry-casting method: mixing active materials with binders and conductive additives such as carbon black and graphite, and then casting the mixture onto a current collector made of metal foil or mesh.<sup>[34–36]</sup> High-efficiency LIBs require active materials with high energy density and minimized amount of non-active components. For this reason, the most commonly used method to obtain a flexible electrode is to settle the active materials onto a flexible conductive substrate without any additives or binders.<sup>[37–41]</sup>

The flexible substrates can be divided into metal,<sup>[29,42,43]</sup> paper and other fabrics,<sup>[26,39,41,44]</sup> and carbon-based materials.<sup>[19,45–48]</sup> Metal substrates that also work as current collectors, such as the most commonly used copper for cathodes and aluminum for anodes, have proved their superior properties of high conductivity, high strength and easy production.<sup>[29,35,49,50]</sup> However, the metal substrates are relatively heavy and smooth, which will decrease the specific capacity of the whole battery. Moreover, the adhesion between the active materials and the metal surface is weak, making the active materials easy to crack and likely to fall off during the bending process.

Non-conductive paper and fabric are explored as substrates due to their good mechanical strength, high flexibility, and low cost.<sup>[26,39,51–56]</sup> Moreover, ordinary paper and fabrics are usually made from fibers such as cellulose, resulting in a rough and porous surface with lots of functional groups. By introducing active materials with high electrical conductivity into ordinary paper or fabric, lightweight and flexible electrodes are obtained for energy storage devices. For example, both cellulose<sup>[39]</sup> and wood fibers<sup>[54]</sup> can be coated with conductive layers of carbon nanotubes (CNTs) to obtain conductive papers as flexible and bendable substrates and electrodes. Other active materials are further added to the conductive paper to increase the capacity of the electrode.<sup>[51,52]</sup> Compared with metal substrates, fabric substrates absorb much more solution, and have a much better adhesion of active materials. This results in a higher mass loading and a significantly improved energy density of the whole battery.<sup>[57]</sup> Furthermore, by paper folding techniques, folded cells based on active powders deposited on paper/CNT substrates displayed an obviously increased area energy density.<sup>[46]</sup>

Conversely, carbon-based substrates including carbon paper, carbon nanofoam, and carbon fabrics show similar advantages to paper and fabric substrates. In addition, they are also electrically conductive.<sup>[58–61]</sup> Novel carbon materials as one-dimensional CNT and two-dimensional graphene are playing

a significant role in the development of flexible energy storage devices, due to their unique properties of light weight, high surface area, high mechanical strength, good electrical conductivity, high chemical and thermal stability and wide potential window.<sup>[62–67]</sup> For example, highly flexible CNT sheets were drawn from CNT arrays to support SnO<sub>2</sub> nanoparticles.<sup>[68]</sup> The obtained binder-free composite electrode showed a reversible capacity of 950 mAh g<sup>-1</sup> after 50 cycles with 0.1C cycling rates. Si/graphene papers were also prepared by dispersing Si nanoparticles on graphene oxide sheets through a filtration method, followed by thermal reduction.<sup>[69]</sup> This composite material showed a high lithium storage capacity of 2200 mAh g<sup>-1</sup> after 50 cycles and 1500 mAh g<sup>-1</sup> after 200 cycles at a current density of 1000 mA g<sup>-1</sup>. It was suggested that a graphene 3D network provided a better electrical contact with Si and served as a mechanically strong framework to support and trap Si active materials during bending and cycling.

Besides being used as conductive and flexible substrates, CNT and graphene have a broad application as additives and active anode materials. Free-standing bare CNT and graphene film usually show anode capacities of 100–600 mAh g<sup>-1</sup>.<sup>[37,63,70–72]</sup> When acting as additives, CNT and graphene are added to non-conductive paper and fabric to result in conductive and flexible substrates, in which they create a three-dimensional network to offer an efficient current transport pathway, a light but strong skeleton and increased surface area for loading active materials.<sup>[73–76]</sup> CNT and graphene-based free-standing composite film electrodes can also be obtained by a variety of methods, such as vacuum co-filtration, blade-coating, self-assembling, dry-drawing, and in-situ growing. In a Si/graphene composite electrode, graphene served as an efficient conducting network to facilitate electrolyte storage and ion diffusion, and accommodated the volume change of Si during the charge-discharge process. It showed a high reversible capacity of 3350 mAh g<sup>-1</sup> at 840 mA g<sup>-1</sup>.<sup>[77]</sup>

The flexibility of the whole battery can be further enhanced by designing some special structures (**Figure 1**).<sup>[46,78]</sup> For example, an origami LIB that can be folded, bent and twisted was produced from a rigid origami technique (Figures 1a and b).<sup>[78]</sup> They were fabricated through the slurry-coating of electrodes onto paper current collectors and encased in standard materials, followed by folding into a Miura pattern. Another cable-typed LIB with high flexibility was produced from hollow-spiral and multiple-helix electrodes, leading to a promising application for future portable and wearable electronics (Figures 1c–f).<sup>[79]</sup> This work has been optimized by replacing the metal wire with CNT composite fibers, which showed a lighter weight and higher volume specific capacity.<sup>[73,80]</sup> Or more recently, after further optimization by introducing novel redox-active catholyte molecules based on 5,12-naphthacenequinone, the resulting LIB showed a significantly improved stability at both room temperature and 60 °C.<sup>[81]</sup>

The other aspect of an LIB lies in the electrolyte. To realize flexible LIBs, one of the most important points is the safety issue and stability during bending. The traditional organic liquid electrolyte suffered from leakage and explosion in flexible LIBs. To this end, the flexible solid-state electrolyte with high ionic conductivity provides a good solution.<sup>[33,82–84]</sup> Adding liquid electrolytes to a polymer is the most commonly used

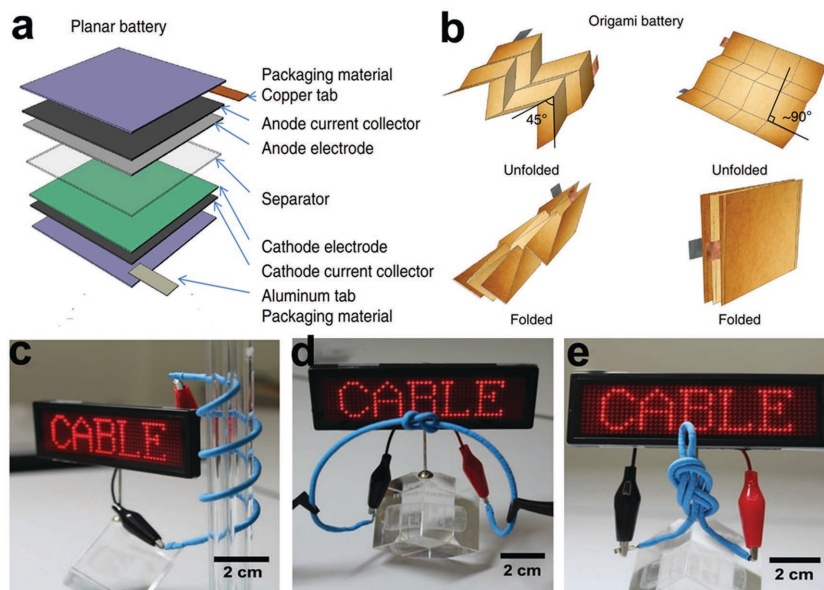


**Figure 1.** Flexible LIBs. a,b) Concept of origami LIBs. Reproduced with permission.<sup>[78]</sup> Copyright 2014, Nature Publishing Group. c–e) A cable-like LIB. Reproduced with permission.<sup>[79]</sup> Copyright 2012, John Wiley and Sons.

method to obtain gel electrolytes, which are leakage-proof with low flammability. Other solid or gel electrolytes such as plastic crystal electrolytes are also widely explored and have been described in detail by other reviews.<sup>[33,85]</sup>

Compared with LIBs, the assembly and structures of SCs are relatively simple. SCs can be water-compatible, and the polyvinyl alcohol (PVA)-based aqueous gel electrolytes are widely explored, e.g., PVA/H<sub>2</sub>SO<sub>4</sub>, PVA/H<sub>3</sub>PO<sub>4</sub>, PVA/KOH and PVA/LiCl.<sup>[86–88]</sup> Other polymers like polyethyleneoxide (PEO) and poly(methylmethacrylate) (PMMA) are also used as polymer matrices for flexible SCs.<sup>[28,89,90]</sup> On the other hand, non-aqueous gel electrolytes consisting of plasticized polymer complexes with electrolytic salts or polar polymer matrices with organic electrolyte solutions can reach a higher voltage of up to 4 V.<sup>[91–93]</sup> Thus the energy density can be greatly increased.

The basic principle of constructing electrodes of flexible SCs is the same as flexible LIBs. What needs to be added is that conducting polymers are more applicable to SCs and are beneficial to flexible electrodes.<sup>[94–98]</sup> Their properties can not only enable an improved flexibility, but commonly used conductive polymers such as polyaniline (PANI), polypyrrole (PPy), poly(3,4-ethylenedioxythiophene) (PEDOT), and their derivatives also show high pseudocapacitance performances. A flexible graphite/PANI hybrid paper electrode exhibited a volume capacitance of 3.55 F cm<sup>-3</sup> at a current density of 4.57 mA cm<sup>-3</sup> and a power density of 0.054 W cm<sup>-3</sup> normalized to the whole volume of the solid-state device.<sup>[99]</sup>

Here, we have summarized the main points concerning the fabrication of flexible LIBs and SCs. It is concluded that each component should be compatible with deformation, which requires a flexible electrode, current collector, and shape-conformable non-liquid electrolyte. By integrating flexible nanostructured materials like CNTs and graphene into conventional rigid electrode materials, flexibility and mechanical stability

are no longer a challenge, but the cost and energy density of the whole device are still not satisfying. A more applicable strategy is still under pressing need with the ever faster development of wearable electronics.

## 2.2. Stretchable Materials

Following the realization of flexible LIBs and SCs, stretchability is the next necessary step to achieve. Wearable electronics require a good adaptability to body movement. However, compared with flexibility, a satisfactory stretchability of a device is much more difficult to obtain. More meticulous designs of both material and structure are required.<sup>[100,101]</sup>

First, the intrinsic stretchable electrode can be developed by using a three dimensional network built by low dimensional materials and restricted by some polymers, such as randomly dispersed CNTs coated on a polydimethylsiloxane (PDMS) substrate.<sup>[102–108]</sup>

In these kinds of electrodes, each low dimensional material has more than one connecting point with each other. When the electrode is being stretched, the low dimensional materials will shift and consequently the connecting points will slip. However, the connections within these low dimensional materials are mostly retained unless they shift too much. The stretchability of the electrode by this method is limited by the size of the low dimensional material and the deformation is difficult to exceed 100%.

Another more universal but efficient method is to deposit active materials onto a stretchable substrate with created wrinkles.<sup>[109–113]</sup> The wrinkles are mostly created by a pre-strain method (Figure 2a). The stretchable substrate is pre-stretched to a certain extent and then coated with suitable active materials prior to release. With the shrinking of the surface area covered with active materials a crumpled morphology is produced. When the electrode is stretched again, within the pre-stretch extent, the wrinkles will be extended and flattened, and the inner structure of the electrodes is not damaged, so that the electrochemical performance is maintained. For instance, a stretchable SC was fabricated by depositing single-walled CNTs onto a pre-stretched PDMS substrate, and the electrical resistances of the buckled single-walled CNT film remained almost unchanged at a strain of up to 140%.<sup>[111]</sup>

An upgrade of the pre-stretch method was developed recently by designing a gum-like structure, and the resulting LIB displayed a significantly improved capability of 400% strain and exhibited stable electrochemical performance after stretching for 500 cycles (Figure 2b).<sup>[114]</sup> Aligned CNT sheets were first stacked on a Cu foil, followed by coating LiMn<sub>2</sub>O<sub>4</sub> or Li<sub>4</sub>Ti<sub>5</sub>O<sub>12</sub> nanoparticles as the cathode and anode, respectively. Later, another CNT sheet was stacked to form a sandwich structure. Afterwards, an un-curing PDMS fluid was introduced into the sandwich structure, which was finally placed onto a 450% pre-stretched PDMS substrate, cured and peeled

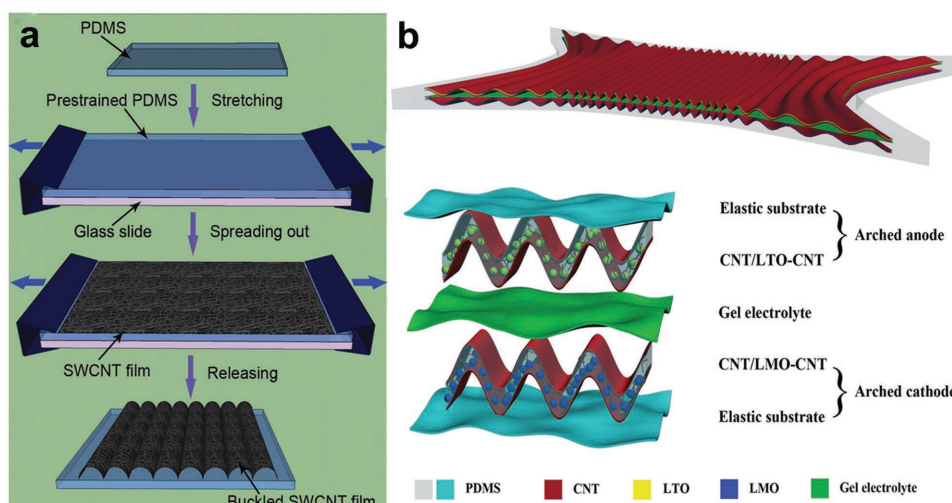


**Figure 2.** Stretchable LIBs based on a wavy structure. a) Schematic illustration of the preparation of a buckled CNT film on PDMS. Reproduced with permission.<sup>[111]</sup> Copyright 2013, John Wiley and Sons. b) Schematic illustration of a super-stretchy LIB and its multi-layered structure. Reproduced with permission.<sup>[114]</sup> Copyright 2015, John Wiley and Sons.

off from the Cu foil. Here a close adherence of the substrate to the sandwich composite was achieved to enable the super-stretchy behavior.

The third method is to bridge rigid materials or components with stretchable interconnections.<sup>[20,115,116]</sup> Thus, the stretchable interconnection parts undertake all the strain and a strong adhesion to the rigid components is important. Au strips that had been patterned on PDMS membranes were connected with rigid Si islands.<sup>[117]</sup> This elastic electronic circuit showed a stretchability of 12% and inspired the following explorations. Recently, the elongation was further increased to 300% through the introduction of a “spring within a spring” structure.<sup>[20]</sup> The LIB included pouch cells where arrays of small-scale storage components were connected by conducting frameworks. It showed a high capacity density of around  $1.1 \text{ mAh cm}^{-2}$ .

A variety of fibers can be also woven into stretchable fabric electrodes,<sup>[118–123]</sup> and they can be stretched to 100–200%. For instance, a stretchable electrode was prepared by immersing the ordinary fabric into a single-walled CNT ink, and the resulting SC can be stretched by 120% 100 times without obvious decay in capacitance. To enhance the energy storage capability, some conducting fibers such as carbon fibers were woven into fabrics for the stretchable SC that did show a high specific capacitance of  $0.5 \text{ F cm}^{-2}$ , but a notable decay in capacitance occurred after bending and stretching by 50%, possibly due to the limited stretchability of carbon fabrics.<sup>[122]</sup>

Recently, considerable attention was attracted to the design of a helically coiled spring to fabricate energy storage devices that were super-stretchy. It can be divided into two main structures. In one case, a fiber electrode or device was shaped into a spring.<sup>[124–128]</sup> Typically, the same two fiber electrodes such as graphene microfibers were coated with a gel electrolyte to obtain a fiber-shaped SC (Figure 3a),<sup>[125]</sup> and the spring-like SC can be then fabricated by wrapping the fiber-shaped SC around a cylinder substrate. As a modification, a spring-like fiber electrode, such as twisted aligned CNT, with coiled loops was first

prepared with a high stretchability of over 300% (Figure 3b).<sup>[129]</sup> An elastic SC was fabricated by placing two spring-like fibers in parallel, while an elastic LIB was produced from two spring-like fibers bearing  $\text{LiMn}_2\text{O}_4$  and  $\text{Li}_4\text{Ti}_5\text{O}_{12}$  nanoparticles as positive and negative electrodes, respectively.

In the other case, active materials are helically wound with an elastic fiber substrate. For instance, a highly stretchable fiber-shaped SC was fabricated by sequentially wrapping aligned CNT sheets on an elastic fiber serving as electrodes (Figure 3c).<sup>[130]</sup> The resulting fiber-shaped SC maintained a specific capacitance of  $18 \text{ F g}^{-1}$  after stretching by 75% for 100 cycles. Later, the same group wound a fiber-shaped cathode and anode in parallel around an elastomer substrate and then coated with gel electrolyte to obtain a super-stretchy LIB which can be stretched by 600% (Figure 3d).<sup>[126]</sup> The stretchability was controlled by the helical angle and the pitch distance of the two fiber-shaped electrodes on the elastic fiber.

Stretchable energy storage devices have been also realized by designing some new architectures including wavy structures, interconnected rigid components through elastic bridges, and textile structures. A variety of methods available for stretchability provides a good adaptability in the design of flexible power systems. More efforts are needed to further enhance the stability of these stretchable energy storage devices and develop matchable packing materials aiming at practical applications in the wearable electronics industry.

### 2.3. Transparent Materials

Transparent materials have attracted increasing attention for various electronic devices including displays, e-papers, touch screens, and smart phones. They are generally realized by coating a thin layer of active materials onto a transparent current collector such as indium tin oxide (ITO)<sup>[21,131–134]</sup> or preparing thin film electrodes in the absence of current

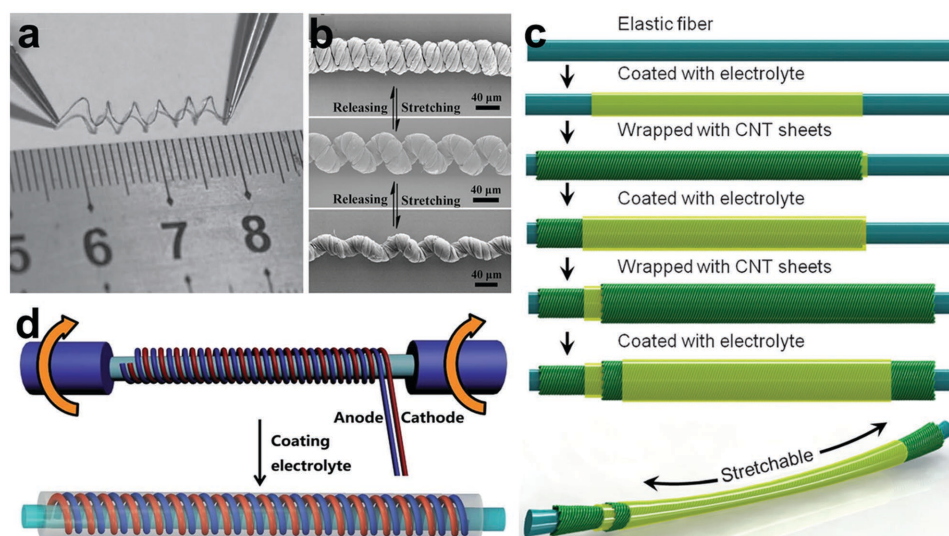


**Figure 3.** Stretchable fiber-shaped energy storage devices. a) A spring-shaped SC. Reproduced with permission.<sup>[125]</sup> Copyright 2013, John Wiley and Sons. b) SEM images of a spring-shaped fiber with increasing strain up to 50%. Reproduced with permission.<sup>[129]</sup> Copyright 2014, John Wiley and Sons. c) Schematic illustration of the fabrication of a highly stretchable, fiber-shaped SC with a coaxial structure. Reproduced with permission.<sup>[130]</sup> Copyright 2013, John Wiley and Sons. d) Schematic illustration of the fabrication of a super-stretchy LIB in a fiber shape. Reproduced with permission.<sup>[126]</sup> Copyright 2014, Royal Society of Chemistry.

collectors.<sup>[108,135–137]</sup> The transparency change of MoS<sub>2</sub> during lithiation/delithiation in a LIB was recently observed in a specially designed microbattery through in-situ transmission electron microscopy.<sup>[138]</sup> The MoS<sub>2</sub> exhibited a bandgap at the range of visible light with low transmittance. The reaction product, Li<sub>2</sub>S, was insulating and expected for high transmittance, and the thin percolative Mo network was also transparent. Therefore, an increased transmittance was produced after lithiation for MoS<sub>2</sub> nanosheets.

A material becomes optically transparent when the thickness is much less than its optical absorption length. Accurately controlled superthin electrode films can be easily prepared with a template method. A Au/MnO<sub>2</sub> core-shell nanomesh structure on a flexible polymeric substrate was produced through a nanosphere lithography combined with an electrodeposition process (Figures 4a–c).<sup>[139]</sup> The efficient contact between the Au current collector and the in-situ grown MnO<sub>2</sub> nanosheet provided excellent electrochemical properties including high capacitance of 4.72 mF cm<sup>-2</sup> with high rate capability besides maintaining a high transparency and flexibility. The similar strategy was also used to fabricate coaxial RuO<sub>2</sub>/ITO nanopillars for a transparent SC, which also showed a maximal specific capacitance of 1235 F g<sup>-1</sup> at a scan rate of 50 mV s<sup>-1</sup>.<sup>[140]</sup>

Recently, some general and promising preparation methods such as spray painting, in-situ growth, and filtration were developed for carbon nanomaterials mainly including CNTs and graphene.<sup>[102,110,135,141–143]</sup> By directly growing graphene films onto a pre-stretched substrate, a stretchable electrode was obtained with an optical transmittance of up to 72.9% at a wavelength of 550 nm, low sheet resistance and desirable mechanical compliance (Figures 4d and e).<sup>[143]</sup> Metal oxides and polymers can be further added to increase the conductivity and capacitance of the carbon-based electrode by co-precipitation and electrochemical deposition, respectively.

## 2.4. Responsive Materials

Energy storage devices with the function to monitor their charging states by exhibiting different colors are promising for various smart devices, and have been recently realized by designing chromatic materials whose colors change under different redox states.<sup>[22,144–147]</sup> An ordered bi-continuous double-gyroid vanadium pentoxide network was developed to make an electrochromic SC (Figures 5a and b).<sup>[144]</sup> An active V<sub>2</sub>O<sub>5</sub> undergoes a reversible Li-ion insertion with colors that changed from yellow to green in two consecutive stages:



Only a fraction of V<sup>5+</sup> ions were reduced to V<sup>4+</sup> ions at the first stage (reduction peak at about 3.4 V) with the color change from yellow to green. The remaining V<sup>5+</sup> ions were reduced to V<sup>4+</sup> ions at the second stage (peak at 3.2 V).

Similarly, metal oxide W<sub>18</sub>O<sub>49</sub> and PANI have also been used as chromatic active materials to constitute the pattern and background in a chromatic SC, respectively (Figure 5c).<sup>[22]</sup> They both revealed high electrochemical and electrochromic behaviors when operated at different ranges of potential windows, i.e., -0.5–0 V for W<sub>18</sub>O<sub>49</sub> and 0–0.8 V for PANI. The cooperation of the two materials enabled the supercapacitor to work at a widened, 1.3 V window while displaying variations in color schemes depending on the level of energy storage. PANI/CNT composite materials were also used to fabricate electrochromic fiber-shaped SCs and stretchable thin-film SCs on the basis of PANI as a chromatic active material.<sup>[145,146]</sup>

Thermally responsive properties have been widely studied to enhance the safety of energy storage devices.<sup>[24,148,149]</sup> High

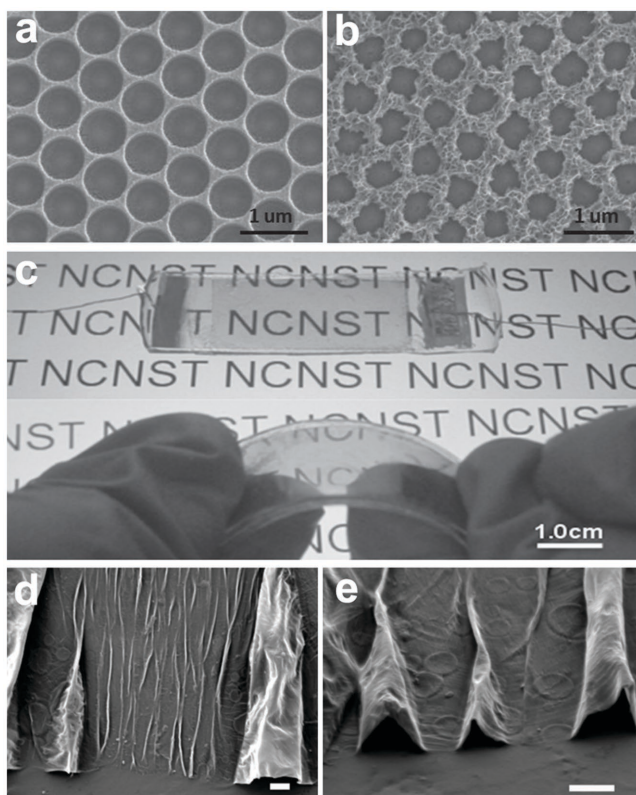


**Figure 4.** Optical devices based on different materials. a,b) SEM images of the Au nanomesh and Au@ $\delta$ -MnO<sub>2</sub> core-shell nanomesh. c) Optical images of a transparent flexible SC based on Au@MnO<sub>2</sub> electrodes sealed in a PDMS film before and after bending. The characters of “NCNST” can be clearly observed below the transparent flexible SC device. Reproduced with permission.<sup>[139]</sup> Copyright 2014, John Wiley and Sons. d,e) SEM images of a four-layered buckled graphene film on PDMS substrate. The scale bars are 1  $\mu$ m at (d) and 20 nm at (e). Reproduced with permission.<sup>[143]</sup> Copyright 2014, American Chemical Society.

power delivery and rapid current flow are prone to generate a severe thermal effect, particularly at high environmental temperatures. The electrochemical power delivery can be commanded by thermally responsive materials, which provide a possible solution to solving this safety vulnerability. For instance, a thermosensitive polymer has been incorporated onto electrodes as active materials to prepare thermally responsive electrodes.<sup>[24]</sup> The configuration of the polymer would change with the varying temperature. The polymer collapsed at 40 °C to inhibit ion transport, and thus weakened the power delivery, while the polymer was dissolved at 20 °C to recover the accessible ion channels for the normal charge-discharge process. Therefore, the resulting SC showed a temperature-triggered on-off capability, i.e., it automatically stopped working at high temperatures.

## 2.5. Self-Healing Materials

Self-healing is an ability to heal and recover from physical damage automatically. This function is particularly desirable for wearable electronic devices that may be damaged with some

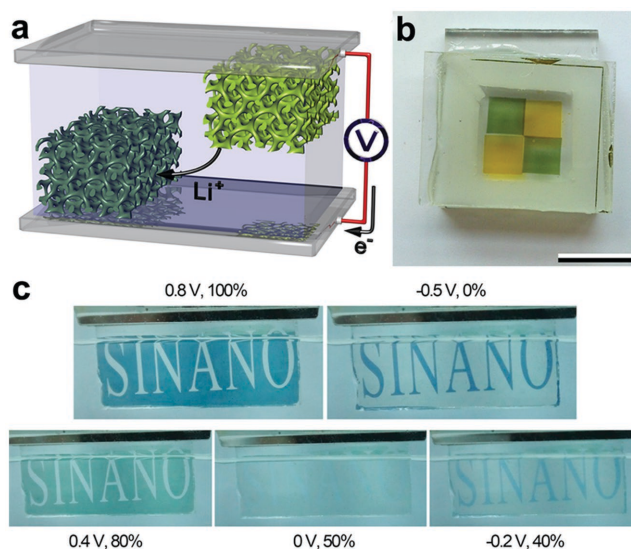


**Figure 5.** Electrochromic SCs. a) Schematic illustration of an SC based on two laterally offset double-gyroid structured electrodes. b) Photograph of a transparent electrochromic SC based on (a). It was composed of an oxidized yellow top electrode, a laterally offset green/gray bottom electrode in the reduced state, and a thermoplastic gasket spacer. Scale bar, 1 cm. Reproduced with permission.<sup>[144]</sup> Copyright 2012, American Chemical Society. c) Photographs of the SC electrode at different states to demonstrate the stored energy conveyed through the patterned color scheme. Reproduced with permission.<sup>[22]</sup> Copyright 2014, American Chemical Society.

severe body movements. Self-healing energy storage devices were generally realized by introducing self-healing materials into active materials.<sup>[23,150–155]</sup> Self-healing materials can effectively work with or without the assistance of external stimuli such as heating or UV light, so they are divided into two general categories, i.e., intrinsic systems based on non-covalent or dynamic covalent attractions and extrinsic systems that need an external healing agent of capsules or vascular networks. Currently, the intrinsic systems are already used in flexible energy storage devices with a self-healing polymer to recover the structure while the active material performs electrochemical storage in the composite.

A typical self-healing composite has been prepared from a supramolecular polymer as host, with inorganic metal particles as nanostructured fillers.<sup>[23,152]</sup> This composite material combined a supermolecular polymeric hydrogen bonding network with glass transition temperatures of below room temperature and nickel microparticles with nanostructured surfaces. The material was flexible and exhibited a conductivity of 40 S cm<sup>-1</sup>. An LIB anode composed of silicon coated with a thin layer of self-healing polymer was made stretchable and could repair spontaneously after mechanical damage and cracks in the composite electrode. Similarly, self-healing polymers could be also incorporated within CNTs to fabricate self-healing SCs. By coating CNTs onto self-healing substrates (composed of a supramolecular network formed through hydrogen bonds and hierarchical flower-like TiO<sub>2</sub> nanostructures) as electrodes, the specific capacitance can be restored up to 85.7% after cutting five times.<sup>[153]</sup> By wrapping CNTs and Ag nanowires onto a self-healing polymer fiber, a self-healable core-shell wire was also

obtained to fabricate a novel fiber-shaped SC.<sup>[155]</sup> It showed a specific capacitance of  $1.34 \text{ mF cm}^{-1}$  and recovered to 92% after breaking and self-healing.

To conclude, energy storage devices have advanced through the introduction of a variety of functional materials into electrodes that have generated new functions besides storing energy. Although flexible, stretchable, transparent, responsive, and self-healing properties are mainly discussed here; other properties such as SCs with alternating current line-filtering functions have been produced to attenuate the leftover alternating current ripples on direct current voltage.<sup>[156,157]</sup> Integration at the level of materials may have different effects on the original electrochemical performances. For instance, after the introduction of CNTs into a rigid material to obtain a flexible electrode, the conductive three-dimensional CNT network reveals a synergistic effect with original electrode active materials, thus increasing the transport efficiency of ions and enhancing the rate capability. On the other hand, the integration of self-healing polymers into active electrode materials decreases the conductivity of the electrode, which decreases the electrochemical properties. This negative influence can be reduced by introducing a third conductive component. However, the increased weight of the electrode still leads to a lower specific capacity. To this end, more efforts are required to design multi-functional composite materials while maintaining high electrochemical performance.

Besides focusing on the functional materials described above, a reasonable connection with other devices is another straightforward way to bring more intelligence into an energy storage system. Among them, integration with energy harvesting devices, which will be discussed carefully below, has successfully realized the self-charging function and turned out to be a promising candidate for powering portable electronic devices.

### 3. Integration at the Level of Devices

Energy harvesting and storage are two critical technologies in energy systems, which are separated units based on different structures and working mechanisms.<sup>[35,158–162]</sup> Due to an intensive demand for miniature and wearable electronics, the development of sustainable and self-powering energy systems has become an important research field. As for rechargeable energy storage devices, LIBs and SCs can store and deliver electric energy through charge and discharge processes. However, the energy storage device must be recharged when the stored energy is depleted. It is not feasible for energy devices used in miniature and wearable electronics to need to be charged from the fixed grid. Thus, it is necessary for energy storage devices to integrate with energy harvesting functions, forming sustainable self-powering energy systems where the incorporated energy harvesting part can charge the energy storage part directly and continuously.

Various energy harvesting parts have been developed and categorized by the harvested energy resources including thermal energy,<sup>[163–165]</sup> solar energy<sup>[158,166,167]</sup> and mechanical energy.<sup>[168,169]</sup> These energy harvesting parts displayed different structures and working mechanisms. Currently, two main kinds of energy harvesting devices, mechanical and solar

energy harvesting devices, have been mostly integrated into energy storage devices.

#### 3.1. Mechanical Energy Harvesting Devices

Mechanical energy, such as vibrational and frictional energy, is a green and ubiquitous resource of nature. Triboelectric and piezoelectric nanogenerators represent the two most explored forms of devices that convert mechanical energy to electrical energy. The mechanical energy is generally intermittent and small due to the irregular and intermittent mechanical motion.<sup>[170–172]</sup> Therefore, it is necessary to store and accumulate the converted electrical energy for applications in electronic devices. Integrating energy storage devices with nanogenerators is studied as a useful strategy with which to achieve the above goal.

##### 3.1.1. Based on the Triboelectric Effect

For a triboelectric nanogenerator (TENG), the working mechanism is based on the conjunction of triboelectrification and electrostatic induction.<sup>[173–175]</sup> Compared to other energy harvesting devices, it can be made with easy processes and low cost, and may output a high power, so it is suitable for the portable electronics. For example, a TENG has been integrated with a flexible LIB to form a wearable power device.<sup>[176]</sup> A Ni-coated polyester belt was prepared as one electrode and the parylene/Ni-coated polyester belt was used as the other electrode. The two electrodes were finally woven into a TENG cloth (**Figure 6a**). The TENG worked through the vertical contact-separation (C-S) motion between the two TENG cloths. As the pressing motion gave rise to a contact electrification, the electrons were transferred from the tribopositive Ni belt to the tribonegative parylene belt. The charge separation generated an electric potential difference (EPD) between the two electrodes. The EPD drove the electrons to transport between the two electrodes through the external circuit. This was reversed during the releasing process (**Figure 6b**). Hence, the pulse current was generated under pressing and releasing. A TENG cloth was integrated with a flexible LIB to form a self-charging device with a rectifier. The generated current was directly conducted to the LIB with the assistance of a rectifier (**Figures 6c–d**). The LIB was charged rapidly to about 1.9 V by the TENG cloth at low-frequency motions (**Figure 6f**). The stored energy was sufficient to power small electronics, such as a heartbeat meter.

##### 3.1.2. Based on the Piezoelectric Effect

Although the TENG can be integrated with LIBs, it required an additional rectifier to convert into a direct current, which is inconvenient for portable applications. To this end, a mechanical-to-electrochemical self-charging power cell (SCPC), where the piezoelectric nanogenerator and the LIB were hybridized into a single device was created (**Figure 7a**).<sup>[177]</sup> The SCPC was fabricated by using a polarized poly(vinylidene fluoride)

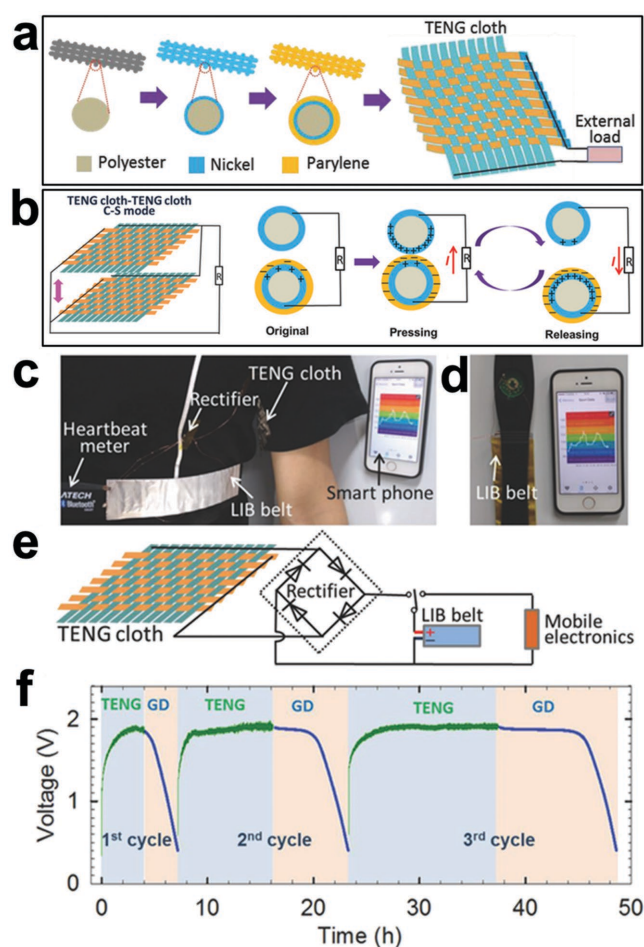


**Figure 6.** Wearable power devices based on TENG and LIB belt. a) Schematic illustration of the fabrication of TENG-cloth. b) Schematic illustration of the working mechanism of the TENG in two TENG cloths with contact-separation mode. c) Photograph of the wearable power device where the TENG-cloth was integrated with LIB to power a heartbeat meter strap that had a remote communication with a smart phone. d) The original coin cell of heartbeat meter being replaced by the LIB belt. e) Equivalent electrical circuit of the power system. f) Typical charge and galvanostatic discharge curve of the integrated device. Reproduced with permission.<sup>[176]</sup> Copyright 2015, John Wiley and Sons.

(PVDF) film to replace the polyethylene separator in the traditional LIB. The entire device was sealed in a stainless-steel coin cell filled with electrolyte (Figure 7b). There were three major parts in the SCPC, i.e., anode, separator and cathode. A Ti foil modified with aligned TiO<sub>2</sub> nanotube arrays acted as an anode and the LiCoO<sub>2</sub>-based composite on the Al foil served as the cathode. A layer of polarized PVDF film between the anode and cathode was used as a separator (Figure 7c). This polarized PVDF separator generated a piezoelectric potential under external stress, which was the driving force for the migration of Li ions.

The working mechanism of the SCPC was involved in an electrochemical process induced by the piezoelectric potential, which was derived from the deformation of PVDF.<sup>[177]</sup> In the original state, it appeared as a discharge state (Figure 7d). When

the SCPC was pressed, a piezoelectric field from the cathode to anode was established in the polarized PVDF (Figure 7e). As a result, the Li ions in the electrolyte were driven by the piezoelectric field, migrating from the cathode to anode. The decreased concentration of Li ions at the cathode enabled the chemical equilibrium ( $\text{LiCoO}_2 \leftrightarrow \text{Li}_{1-x}\text{CoO}_2 + x\text{Li}^+ + x\text{e}^-$ ) to move to the right. In this case, the Li ions were de-intercalated from LiCoO<sub>2</sub> to form Li<sub>1-x</sub>CoO<sub>2</sub> at the cathode electrode. Meanwhile, the increased concentration of Li ions at the anode produced Li<sub>x</sub>TiO<sub>2</sub> according to the chemical equilibrium ( $\text{TiO}_2 + x\text{Li}^+ + x\text{e}^- \leftrightarrow \text{Li}_x\text{TiO}_2$ ) (Figure 7f). During the above process, the Li ions were continuously migrated from the cathode to anode and the device was charged until the piezoelectric field was balanced by the transferred Li ions. In a self-charging and discharging cycle of the SCPC, the voltage of the device was increased by 65 mV within 4 min under pressing (Figure 7g). After finishing the self-charging process, the SCPC can be discharged to the original voltage. The stored electric capacity was ≈0.036 μAh.

The performance of the SCPC was affected by the pressing force and the used materials. The increasing force and frequency can both enhance the self-charging effect. Under the same force, a flexible device can generate a higher piezoelectric performance than a rigid one due to the larger deformation. A flexible Kapton film was used as a substrate to fabricate the flexible SCPC.<sup>[178]</sup> The flexible SCPC exhibited a better self-charging effect compared to the rigid SCPC based on a stainless steel substrate. Minute mechanical forces such as those produced by the pressing of fingers can provide enough strain for this flexible SCPC. In view of the fact that mechanical energy harvesting and storage mainly relied on the piezoelectric field generated in the PVDF separator, optimizing the structure of the piezoelectric separator is an effective way to improve the performance. For instance, a porous structure was designed for the PVDF separator using ZnO nanowire arrays as templates.<sup>[179]</sup> This porous structure can facilitate the transport of Li ions, leading to a higher performance. In order to effectively use the piezoelectric field, some composite materials such as CuO/PVDF nanocomposites were synthesized as the anode by infiltrating the PVDF gel into the grass-like CuO nanoarrays.<sup>[180]</sup> In this composite, the intimate and large contact between CuO nanoarrays and PVDF gave the integrated device a high performance compared to the previous structure in which the prepared PVDF film was merely deposited onto the CuO arrays.

### 3.2. Solar Energy Harvesting Devices

Solar energy is a widespread, renewable, and environmentally-friendly resource in the world. To utilize solar energy in our daily life, solar cells have been mostly developed for harvesting solar energy and further converting it to electrical energy. In view of the variation in sunlight intensity under different weather conditions, locations, and times, the energy output of the same solar cell may fluctuate, and it is therefore not suitable for direct use in electronic devices.

Energy storage devices including LIBs and SCs can effectively store electrical energy. An effective approach to



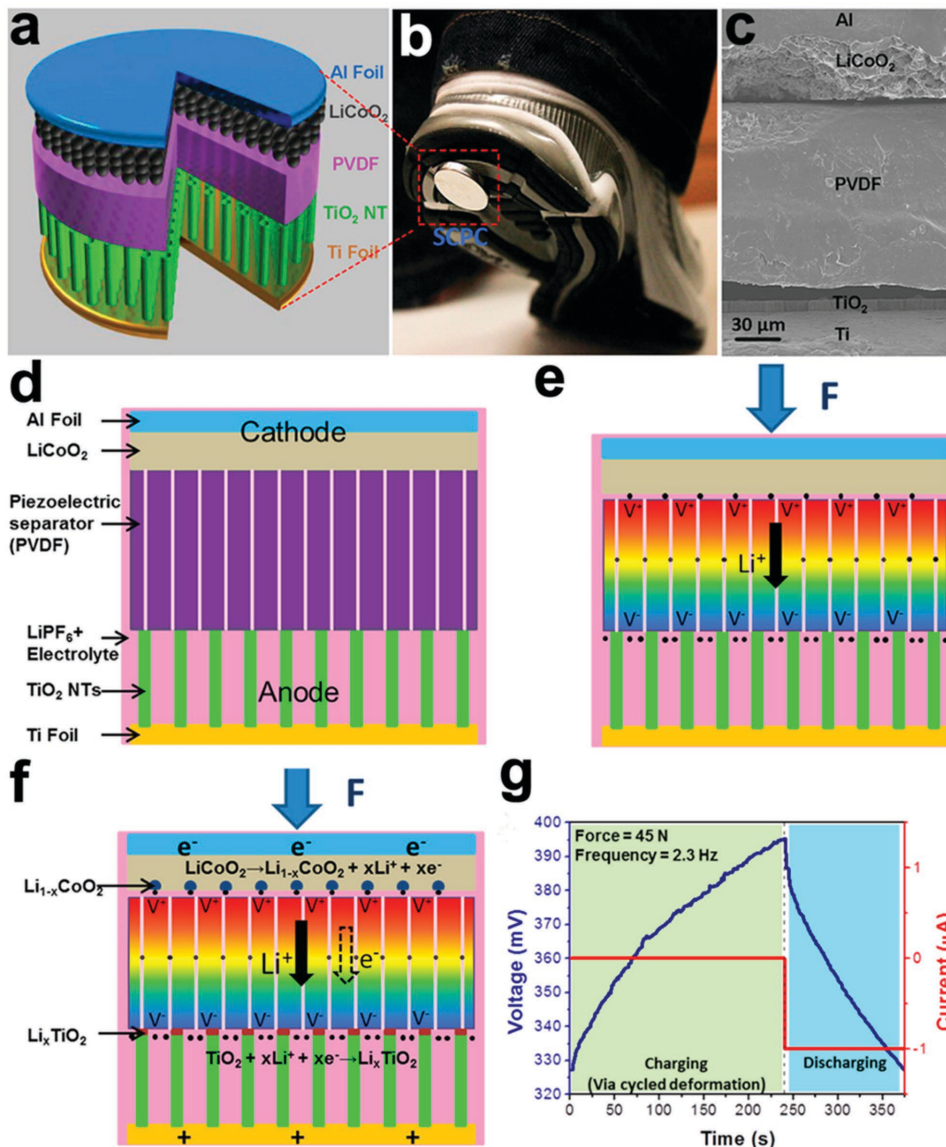


**Figure 7.** a) Schematic illustration of the self-charging power cell (SCPC) by hybridizing a piezoelectric nanogenerator and an LIB. b) Sticking an SCPC on the bottom of a shoe for harvesting and storing the compressive energy generated by walking. c) Cross-sectional SEM image of the SCPC. d) Schematic illustration of the SCPC in a discharged state. e) Schematic illustration of the piezopotential generated after a compressive stress was applied to the SCPC. f) Schematic illustration of the corresponding charging reaction of the SCPC. g) A typical curve of self-charging and galvanostatic discharge for the SCPC. Reproduced with permission.<sup>[177]</sup> Copyright 2012, American Chemical Society.

collecting the fluctuating electricity generated from solar cells is to integrate solar cells and energy storage devices, i.e., the solar cell part charges the energy storage part instead of the power grid. Therefore, the converted electrical energy from the solar cell can be effectively stored, to not only avoid energy waste, but also to make the output power stable. Currently, energy storage units have been successfully integrated with silicon solar cells, polymer solar cells (PSCs) and dye-sensitized solar cells (DSSCs) to form self-charging energy devices.<sup>[181–187]</sup> The performance of the integrated energy device is determined by the photovoltaic conversion and energy storage part, and the entire energy conversion and

storage efficiency is calculated by multiplying power conversion and energy storage efficiencies.

For both photovoltaic conversion and electrochemical storage parts, the electrode materials are a key to their performances. The photovoltaic conversion part includes two electrodes for transferring and collecting charges, and the electrochemical storage part also needs two electrodes with an electrolyte typically sandwiched between them. The two parts are generally connected through external conductive wires with low efficiencies. It is difficult or even impossible to make such a connection for various miniature and portable electronic devices. Therefore, the integration of the above two functions into one

device has become standard in recent years. The energy harvesting and storage parts typically share one or two electrodes in the integrated device.

### 3.2.1. Planar Shaped Devices

The integrated energy device realizes energy conversion and storage in one device. The traditional configuration is a planar shape, in which it is easy to integrate these two parts into one unit. Due to the low cost and easy fabrication, DSSCs are firstly integrated with LIBs or SCs. A DSSC is composed of a working electrode, a counter electrode and an electrolyte. The counter electrode is opaque, so a DSSC is usually illuminated from the working electrode. One electrode of the LIB or SC part may share the counter electrode with the DSSC, so the design of the shared electrode is a key to the performance of the integrated energy device. For instance, a platinum sheet with one side being coated by an activated carbon layer was prepared as such an effective electrode.<sup>[188]</sup> The activated carbon layer served as an electrode material of the SC, while the uncovered platinum side functioned as a counter electrode of the DSSC. The shared electrode was assembled with a dye-sensitized TiO<sub>2</sub> layer working electrode and an activated carbon layer to form the DSSC and SC part, respectively. As expected, in this integrated energy device, the electrical energy generated from the DSSC part was directly stored in the SC part.

Besides the metal electrode, a variety of nanostructured electrodes based on carbon nanomaterials such as CNT have

also been widely explored as sharing electrodes due to their high electrocatalytic activities in DSSCs and high long-term stability as electrodes in SCs.<sup>[189–194]</sup> For instance, a flexible, free-standing and aligned multiwalled CNT sheet was prepared as a sharing electrode in an integrated energy device (Figure 8a).<sup>[195]</sup> When the working electrode of a DSSC part was connected with the other electrode of the SC part, the voltages of the integrated device were increased rapidly under illumination, indicating the charging process. The voltage was maintained at 0.72 V, which was slightly lower than the open-circuit photovoltage of the DSSC unit, due to the electricity lost in the external circuit (Figures 8b and c). After finishing the charging process, the stored electrical energy can be outputted under galvanostatic discharging when the SC part was connected to the external load. The SC part can be charged again by the DSSC part when the DSSC part was illuminated. For the integration of solar cells and SCs, it is critically important to enhance the specific capacitance of the SC, aiming at improving the storage capability of the integrated energy device. The introduction of a second phase with high electrochemical properties represents the most studied strategy for the SC part. Both metal oxides and conducting polymers have been extensively investigated. For instance, the pseudocapacitive PANI has been infiltrated into the aligned CNT sheet, and the output electric power of the integrated energy device was greatly enhanced (Figure 8d).<sup>[195]</sup>

Generally, the output voltage was below 1.5 V when SCs are integrated with solar cells. There are two methods to obtain high output voltages from integrated devices. In one case, the integrated devices can be connected in series. For example,

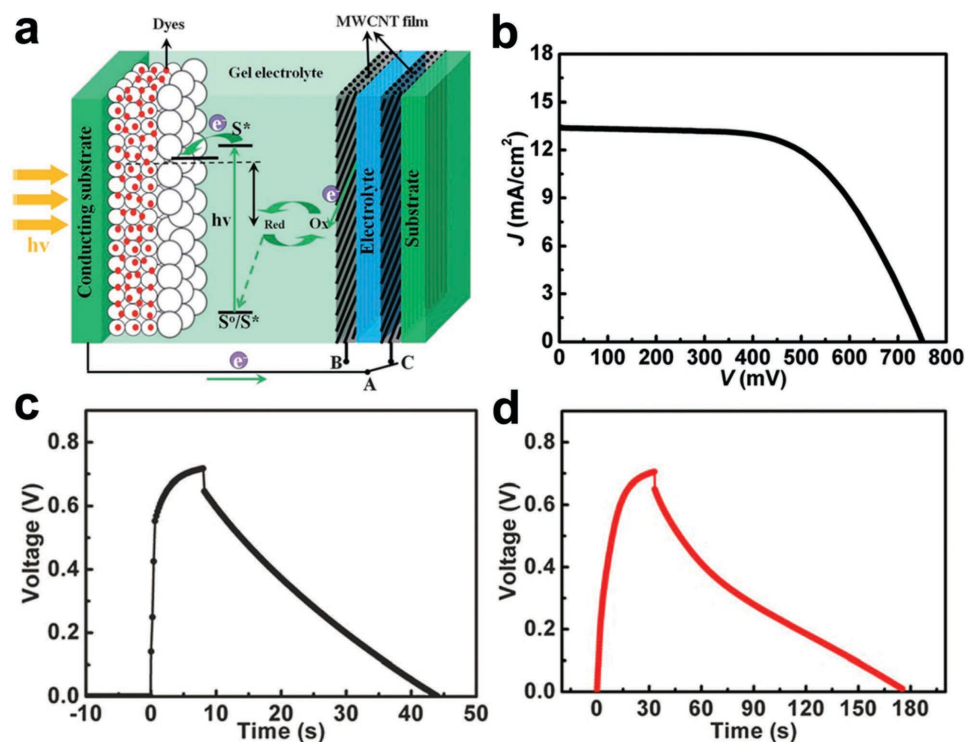


**Figure 8.** The integrated DSSC and SC device. a) Schematic illustration of an integrated device. b) Photocurrent density–voltage characteristics of an integrated device. c,d) Photocharging and galvanostatic discharging curves of integrated devices with bare multi-walled CNT sheets and multi-walled CNT/PANI composite films as electrodes, respectively. Reproduced with permission.<sup>[195]</sup> Copyright 2013, Royal Society of Chemistry.

four integrated devices were arranged in series to output a higher voltage of 2.5 V.<sup>[196]</sup> In the other case the energy storage part with a higher voltage, such as LIB, may be used to replace the SC. An output voltage of  $\approx 3$  V had been achieved through this strategy.<sup>[197]</sup> To prepare the sharing electrode, aligned TiO<sub>2</sub> nanotube arrays were grown at both sides of a Ti foil with one side as a working electrode of DSSC part and the other side as the anode of LIB part (Figure 9a). When the DSSC part was illuminated, the generated electrons transported along the Ti foil to the anode where the following reaction occurred, i.e.,  $(\text{TiO}_2 + x\text{Li}^+ + xe^- \leftrightarrow \text{Li}_x\text{TiO}_2)$ . At the cathode, another reaction occurred to release the electrons, i.e.,  $(\text{LiCoO}_2 \leftrightarrow \text{Li}_{1-x}\text{CoO}_2 + x\text{Li}^+ + xe^-)$ . The electrons reached the counter electrode of the DSSC part through the external circuit to combine with the holes at the counter electrode (Figure 9b). Under continuous illumination, the Li ions were inserted into the anode to realize a charging process. The voltage of a single DSSC unit is about 0.8 V, which does not match the voltage platform of the LIB part. Therefore, four tandem DSSCs were used as energy harvesting units to charge the LIB. The voltage of the integrated device was increased to 3 V in  $\approx 8$  min, and the stored electric capacity was about 33.89  $\mu\text{Ah}$  according to the discharging process (Figure 9c). The performance of the

integrated device can be well maintained after three cycles of the charging and discharging processes. Moreover, the stored energy in this integrated device can effectively power small electronic devices such as light-emitting diodes (LEDs).

Both DSSC and LIB, or SC parts require different electrolytes, usually liquid electrolytes that are inconvenient, or even have problems such as leakage and volatilization. Therefore, it is necessary to further seal such integrated energy devices for practical applications. Gel electrolytes have been thus proposed to fabricate solid-state DSSCs and the following integrated energy devices, though both mechanical and thermal stability need to be further enhanced. To this end, solid-state solar cells and SCs have been widely investigated to form an all-solid-state integrated energy device.<sup>[198]</sup>

### 3.2.2. Fiber Shaped Devices

The planar device is usually heavy, rigid, and large, restricting their applications to portable electronics. Recently, fiber-shaped energy devices were developed for applications in portable and wearable electronics due to their flexibility, light weight and weaving properties.<sup>[199–219]</sup> The explored fiber-shaped energy devices mainly contain energy harvesting and storage devices. Integrating fiber-shaped SCs/LIBs with solar cells to form fiber-shaped integrated energy devices can realize self-powering and portable applications simultaneously.<sup>[220–224]</sup>

Aligned CNT fibers have been widely investigated for the fabrication of fiber-shaped integrated devices. For instance, an SC and a DSSC were assembled into one device based on a TiO<sub>2</sub> nanotube-modified Ti wire as the sharing electrode.<sup>[220]</sup> Two aligned CNT fibers were twisted around the Ti wire to form the DSSC and SC parts (Figures 10a–e). The aligned TiO<sub>2</sub> nanotubes can effectively enhance charge separation and transport for the DSSC and enlarge the contact area with electrolytes for the SC. The flexible CNT fiber ensured a good contact with the modified Ti wire in each part. During the charging process, the DSSC and SC part were bridged together by connecting the two separated CNT fibers. The generated electrons from the DSSC part can be directly stored in the SC part, and the voltage was increased rapidly to 0.6 V, which was close to the open-circuit photovoltage of the DSSC (Figures 10f and g). The entire energy conversion and storage efficiency was appropriately 1.5%, where the power conversion efficiency was 2.2% and the storage efficiency was 68.4%.<sup>[220]</sup>

By combining the characteristics of fiber shape and planar architecture, a coaxial structure offers some advantages compared to the twisting structure in the fiber-shaped device, e.g., the contact between the electrode and electrolyte were better with a higher stability.<sup>[225–227]</sup> Coaxial fiber-shaped integrated energy devices have been also created recently by introducing appropriate electrode materials. A flexible, transparent, conductive CNT sheet has been found to effectively meet the requirements. A modified Ti wire as the sharing electrode was wrapped by two separated CNT sheets with one as the counter electrode for DSSC and the other as an electrode for SC. This coaxial integrated device showed high stability, and the entire energy conversion and storage efficiency can be maintained at 88.2% after bending for 1000 cycles.<sup>[223]</sup>

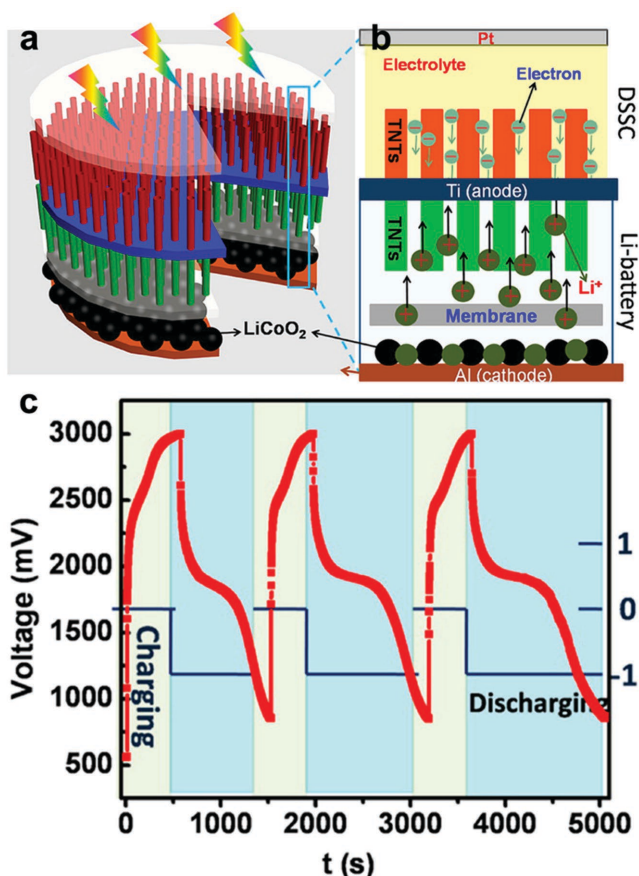


**Figure 9.** The integrated DSSC and LIB device. a) Schematic illustration of an integrated device. b) Detailed structure and working mechanism of the integrated device. c) The discharge/charge cycling curves of the integrated device with four tandem DSSC units and one LIB unit. Reproduced with permission.<sup>[197]</sup> Copyright 2012, American Chemical Society.

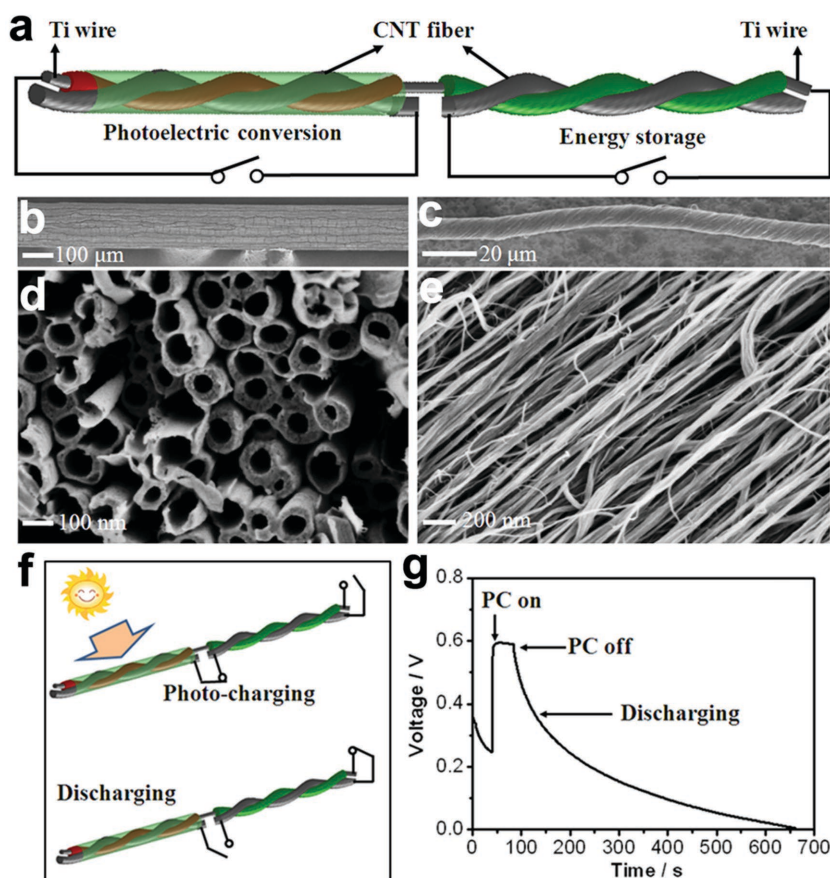


**Figure 10.** The fiber-shaped integrated device based on DSSC and SC. a) Schematic illustration of a fiber-shaped integrated device. b) SEM image of a shared Ti wire electrode grown with  $\text{TiO}_2$  nanotube arrays on the surface. c) SEM image of a CNT fiber. d, e) Enlarged views of (b) and (c), respectively. f) Schematic illustration of the electrode connection during charging and discharging. g) Photocharging-discharging curve of a fiber-shaped integrated device. Reproduced with permission.<sup>[220]</sup> Copyright 2012, John Wiley and Sons.

As previously mentioned, for the integration of liquid-based fiber-shaped DSSCs into the LIB or SC, it is necessary to seal them for stable performance, which is complex and inconvenient for applications. Therefore, the development of an all-solid-state solar cell that can work in air becomes critically important for low cost and high stability. To this end, polymer solar cells (PSC) represent a promising candidate to satisfy them. An all-solid-state integrated energy fiber has been designed and fabricated from a PSC and an SC (Figure 11a).<sup>[222]</sup> A Ti wire was first grown with a layer of aligned  $\text{TiO}_2$  nanotube arrays. The left part of the modified Ti wire was then sequentially coated with poly(3-hexyl thiophene):phenyl-C61-butryric acid methyl ester (P3HT:PCBM) and poly(3,4-ethylenedioxythiophene):poly(styrene sulfonate) (PEDOT:PSS) on the surface, followed by winding the aligned CNT sheet to form the PSC unit. Afterwards, the right part of the modified Ti wire was wrapped by another CNT sheet, followed by coating a layer of poly(vinyl alcohol) (PVA)/ $\text{H}_3\text{PO}_4$  gel electrolyte to form the SC. A single layer of CNT sheet was preferred to obtain the best performance for the PSC part. For this integrated device, the entire energy conversion and storage efficiency was gradually increased with increasing CNT sheet thickness in the

SC part. A maximal entire efficiency of 0.84% was achieved at a thickness of 20  $\mu\text{m}$ . This all-solid-state integrated energy device displayed a high stability with the entire energy conversion and storage efficiency being maintained at over 90% after bending for 1000 cycles (Figure 11b). Furthermore, this integrated energy fiber can effectively work and may be stored without sealing, and the entire efficiency can be maintained at 75% in 7 days (Figure 11c).

Perovskite solar cells represent one of the most explored solid-state solar cells and have started to attract increasing attention for their high power conversion efficiencies.<sup>[228–235]</sup> Recently, fiber-shaped perovskite solar cells have been realized through the use of modified Ti wire and aligned CNT sheets as two electrodes with the perovskite material sandwiched between them.<sup>[236]</sup> After modification by introducing an elastic fiber substrate according to the strategy in DSSCs,<sup>[237]</sup> the resulting fiber-shaped perovskite solar cell can be further made to be stretchable. Similar to the DSSC, the perovskite solar cell should also be able to be integrated with the SC or LB into a fiber shape. However, it remains unavailable and may attract increasing attention in the near future, particularly considering that integrated devices showed low efficiencies while the perovskite solar cells exhibited the promise of high power conversion efficiencies.

To conclude, by integrating energy storage devices with energy harvesting devices, self-charging power systems can be successfully realized in both planar and fiber shapes. The utilization of mechanical energy from body moments and solar energy from daylight, provide a promising option for renewable and sustainable power systems, especially aiming at miniature equipment. Based on the integrated energy storage devices described above, efforts have been further paid to develop novel power fabrics that represent a new platform in the advancement of energy storage.

#### 4. Integrated Energy Storage Fabrics

Emerging research on portable power devices has aroused tremendous interest in wearable energy systems. Although LIBs and SCs are desirable power devices for future portable, wearable and miniature electronic devices, their traditional bulky shape still cannot meet the future needs. To this end, increasing interest has been attracted to making energy storage fabrics, as a promising future direction. So far, the energy storage fabrics can be fabricated by two methods. One is made from custom fabrics. The other one is woven from fiber-shaped energy storage devices.

Custom fabrics, including cotton and polyester fabrics, are low-cost and easily obtained. The original non-conductivity of

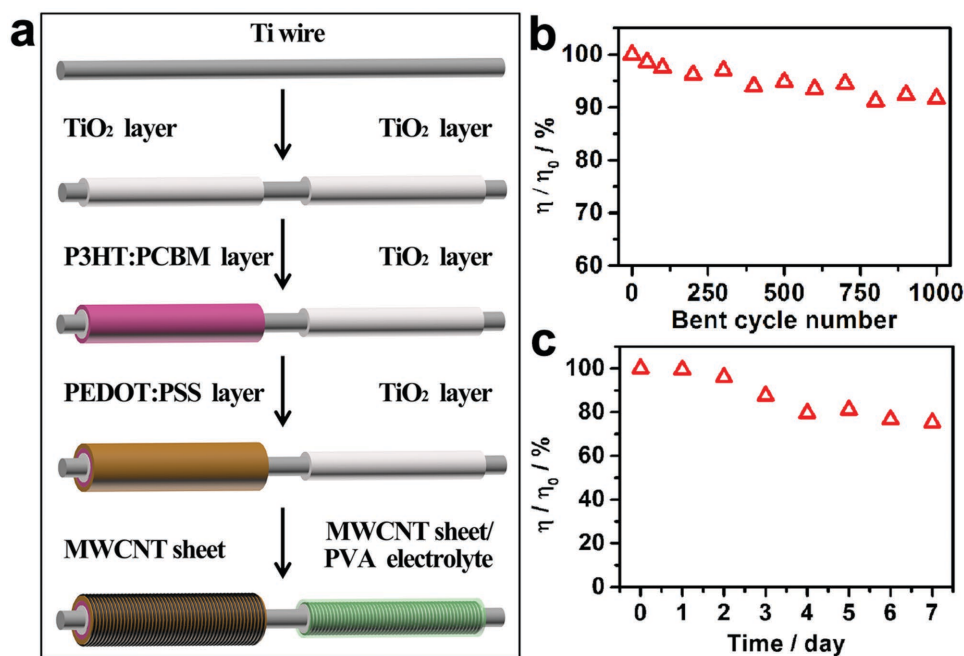


**Figure 11.** A fiber-shaped integrated device based on PSC and SC. a) Schematic illustration of the fabrication process. b) Dependence of the entire energy conversion and storage efficiency of integrated device on bent cycle number. c) Dependence of the entire energy conversion and storage efficiency of integrated device on time. Reproduced with permission.<sup>[222]</sup> Copyright 2014, John Wiley and Sons.

these fabrics restricts their application as electrode materials. Hence, conductive materials are introduced to prepare a conductive fabric. Due to electrical conductivity and stable energy storage performance, activated carbon, CNT, and graphene are incorporated into the fabric through various methods including dip-coating, screen-printing and bush-coating.<sup>[26,121,238–240]</sup> For instance, a conductive fabric was prepared by dipping the cotton cloth into a single-walled CNT ink. The produced fabric showed a high electrical conductivity and the sheet resistance was less than  $1 \Omega \text{ sq}^{-1}$ .<sup>[121]</sup> Using this conductive fabric as both active material and current collector, a high-performance flexible SC fabric was obtained. A cotton fabric could be also modified with the other carbon nanomaterials such as graphene. Using a simple brush-coating method with graphene oxide ink, a conductive graphene-cotton fabric was produced after annealing. The SC fabric had a specific capacitance of  $81.7 \text{ F g}^{-1}$ .<sup>[239]</sup> Aside from incorporating conductive carbon-based materials, custom fabric can be also converted into conductive fabric by a direct activated process.<sup>[241,242]</sup> For example, a cotton cloth was converted into activated carbon fabric by the chemical active procedure and heating treatment. The original 3D porous microstructure was well maintained after coating capacitive materials such as  $\text{MnO}_2$ , which was beneficial to the electrolyte infiltration.<sup>[242]</sup>

A custom fabric is made up of yarns, so the conductive yarns can be directly woven into a conductive fabric. An energy storage fabric can be obtained by coating electrolyte onto this fabric. Activated carbon materials were introduced into swelled yarns, including cotton, linen, bamboo, and viscose yarns, through fiber welding.<sup>[243]</sup> The introduced carbon particles cover the surface of the fiber, forming a conductive network among welded fibers. These composite yarns can be

successfully woven into a fabric with non-conductive yarns that act as a physical separator (Figure 12a). The gel electrolyte was finally coated onto the fabric to form the SC. This SC fabric showed a flexibility and elasticity (Figure 12b). When the single yarn was twisted with a steel wire to form the carbon/steel yarn, a higher performance SC fabric was achieved due to the higher electrical conductivity of the carbon/steel yarn.

Alternatively, the conductive yarn can be used in fiber-shaped energy devices, which can be then woven into energy fabrics. Hence, the fiber-shaped device plays a vital role in obtaining high performance fabrics. Carbon-based fibers, including CNT, graphene, and composite fibers, are promising electrodes in fiber-shaped SCs. For instance, a fiber-shaped SC based on a single-walled CNT fiber was obtained by twisting two fiber electrodes together, and the final SC was integrated into traditional cloth to form an energy storage fabric (Figure 12c).<sup>[244]</sup> Compared with SCs, LIBs have a higher energy density, which is beneficial for high performance fabric. A fiber-shaped LIB was obtained by twisting the CNT/ $\text{MnO}_2$  composite fiber and a Li wire as positive and negative electrodes, respectively.<sup>[73]</sup> Using the metal Li wire is not welcome for practical applications. In order to improve flexibility and safety, a coaxial full LIB based on CNT/ $\text{LiMn}_2\text{O}_4$  and CNT-Si/CNT composite fibers was developed. This full LIB can be woven into an energy storage fabric with an area energy density of  $4.5 \text{ mWh cm}^{-2}$  (Figure 12d).<sup>[27]</sup> When the energy device is integrated into cloth, it is inevitably folded and stretched, so developing a highly stretchable energy device is important for their stable operation. Accordingly, a fiber-shaped LIB with an elongation of 600% was integrated with a cloth. This energy fabric can well perform during folding and stretching of the cloth (Figures 12e–h).<sup>[126]</sup>

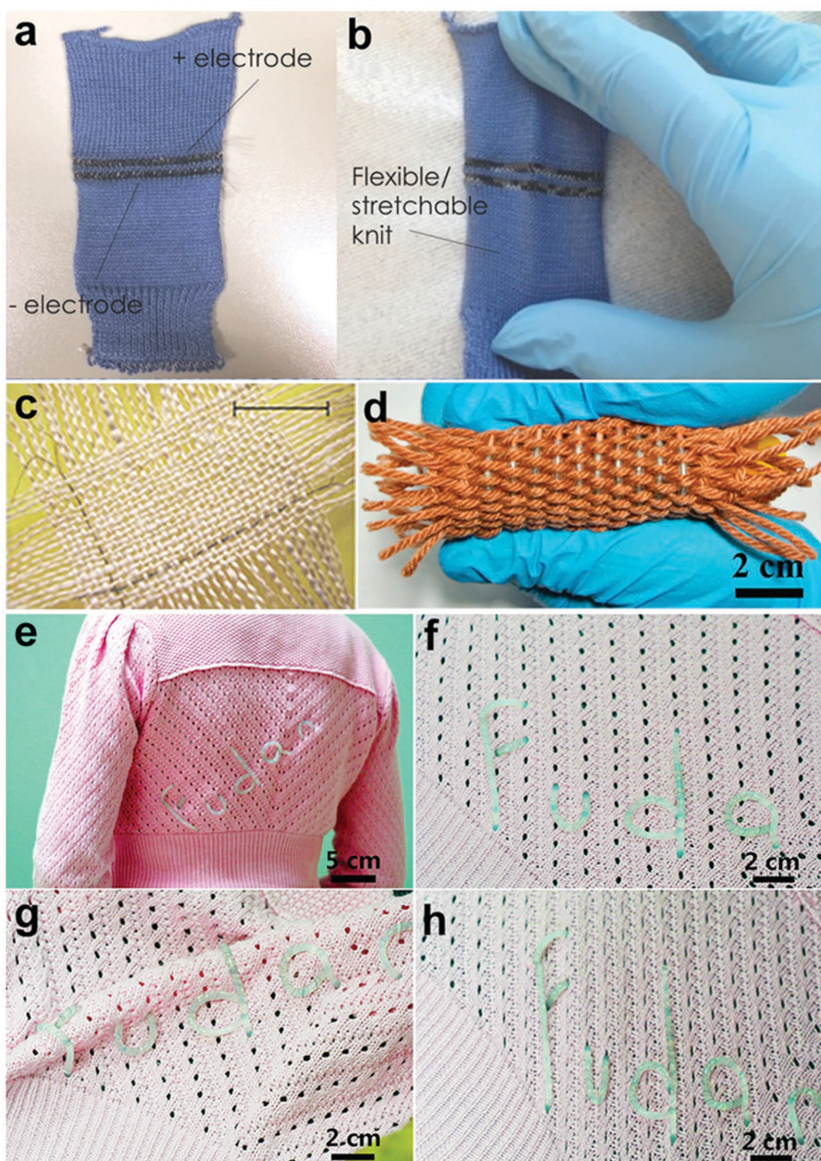


**Figure 12.** Power fabrics based on LIB and SC. a) Photograph of a flat knitted SC. b) Photograph of knitted SC under stretching. Reproduced with permission.<sup>[243]</sup> Copyright 2015, John Wiley and Sons. c) Photograph of fiber-shaped SCs being woven into a fabric. Scale bar, 1 cm. Reproduced with permission.<sup>[244]</sup> Copyright 2003, Nature Publishing Group. d) Photograph of fiber-shaped full LIBs being woven into a fabric. Reproduced with permission.<sup>[27]</sup> Copyright 2014, American Chemical Society. e–h) Photographs of stretchable fiber-shaped LIBs being woven into a sweater (e and f) under folding (g) and stretching (h). Reproduced with permission.<sup>[126]</sup> Copyright 2014, Royal Society of Chemistry.

Aside from outputting power, the energy fabric can be endowed with other functions. For example, a smart SC was fabricated based on an electrochromic fiber where a CNT-based fiber was coated with PANI.<sup>[146]</sup> Different colors of fiber electrodes, derived from different oxidation states of PANI, can be shown under different voltages (Figures 13a–e). These electrochromic fibers were easily woven into a fabric. When some fibers in the fabric were selected as positive electrodes and other fibers were used as negative electrodes, some specific symbols, according to the selective electrodes, can be displayed

during charging/discharging processes (Figures 13f–h). The alterable colors in this system were light yellow, blue and green. Other colors may be also realized as long as different polymers and inorganic oxides are introduced.

## 5. Conclusions and Outlook

To satisfy the increasing energy demands for portable, wearable and miniature electronic devices, it is necessary to develop high-performance energy storage systems. Apart from the basic function of storing electrical energy, additional functions have been incorporated into energy storage devices. Integration has proven to be an effective strategy for improving the performance of energy storage devices. Flexibility, stretchability, transparency, electrochromism, intelligence, and self-healing functions have successfully been introduced into LIBs and/or SCs. Moreover, energy storage devices can be integrated with energy harvesting devices, including nanogenerators and solar cells, to form self-powering energy systems. To effectively harvest and store energy, the energy harvesting and energy storage unit need to be well matched and delicately designed. These integrated energy devices can harvest energy from the environment and store energy simultaneously, with promising applications to portable electronic devices. The flexible, lightweight, and weavable fiber-shaped energy devices are easily integrated with fabric to form energy powering fabrics that show promising applications for wearable electronics.

Although some functional energy storage devices have been well designed and show good prospects, they are still below the performance requirements for next-generation electronics. Some aspects may be improved by future study of the following aspects. 1) Integrating two or more functions into one energy storage device is necessary. This becomes more complex for future portable electronic devices. Developing multifunctional energy storage devices is effective for reducing the component amount with a smaller size. 2) It is necessary to optimize the structure of integrated energy harvesting and storage devices. Nowadays, integrated energy devices are usually fabricated by sharing one electrode. Hybridizing energy storage and harvesting device into single device is a useful way to reduce the device volume. Taking the integrated DSSC and SC device for an example, it is necessary to invent a sharing electrolyte that is applicable to both parts. 3) As for fiber-shaped energy storage devices, a

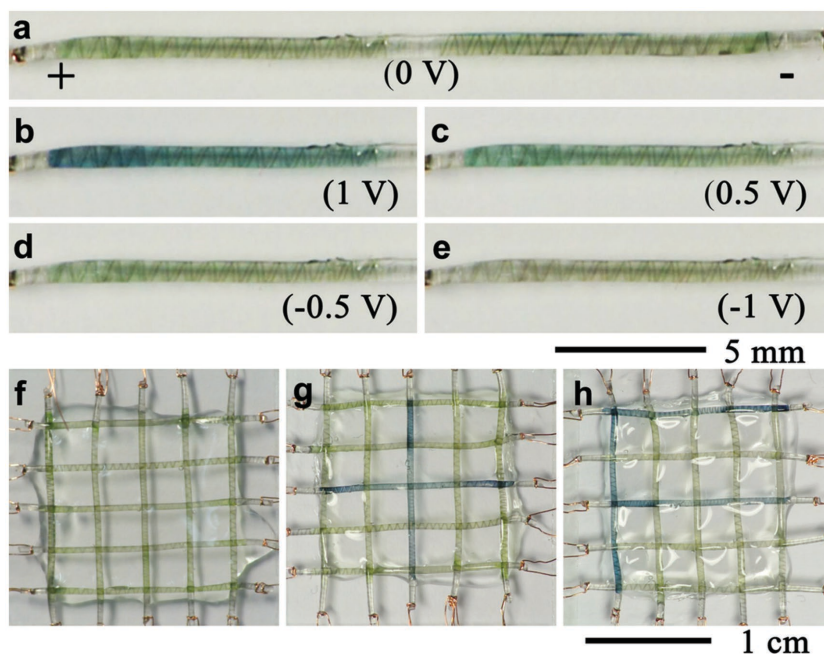


**Figure 13.** Electrochromic SC fabric woven from electrochromic fibers. a) An electrochromic fiber-shaped SC at 0 V. b–e) Positive electrode at 1, 0.5, –0.5 and –1 V, respectively. f) An SC fabric woven from electrochromic fibers. g,h) Photographs of the signs of “+” and “F” in the electrochromic SC fabric. Reproduced with permission.<sup>[146]</sup> Copyright 2014, John Wiley and Sons.

longer device should be developed for power fabric. To date, most lab-made fiber-shaped devices are at centimeter-scale and the performance degrades sharply when the length is extended. The conductivity of the fiber electrode is a critical factor for scaling up. Hence, developing a high conductivity and electrochemical activity fiber electrode is a main direction for the next stage of research.

## Acknowledgements

S.P. and J.R. contributed equally to this work. This work was supported by NSFC (21225417, 51403038), MOST (2011CB932503), STCSM (15XD1500400), Changjiang Chair Professor Program and the Program for Outstanding Young Scholars from Organization Department of the CPC Central Committee.

Received: September 17, 2015

Revised: November 6, 2015

Published online:

- [1] Y. Chen, J. Au, P. Kazlas, A. Ritenour, H. Gates, M. McCreary, *Nature* **2003**, 423, 136.
- [2] S. Bauer, *Nat. Mater.* **2013**, 12, 871.
- [3] M. Kaempgen, C. K. Chan, J. Ma, Y. Cui, G. Gruner, *Nano Lett.* **2009**, 9, 1872.
- [4] G. Nystrom, A. Marais, E. Karabulut, L. Wagberg, Y. Cui, M. M. Hamedi, *Nat. Commun.* **2015**, 6, 7529.
- [5] M. Winter, J. O. Besenhard, M. E. Spahr, P. Novak, *Adv. Mater.* **1998**, 10, 725.
- [6] J. B. Goodenough, Y. Kim, *Chem. Mater.* **2010**, 22, 587.
- [7] Y. Gogotsi, P. Simon, *Science* **2011**, 334, 917.
- [8] P. J. Hall, M. Mirzaei, S. I. Fletcher, F. B. Sillars, A. J. R. Rennie, G. O. Shitta-Bey, G. Wilson, A. Cruden, R. Carter, *Energy Environ. Sci.* **2010**, 3, 1238.
- [9] V. Etacheri, R. Marom, R. Elazari, G. Salitra, D. Aurbach, *Energy Environ. Sci.* **2011**, 4, 3243.
- [10] Z. Chen, Y. Qin, D. Weng, Q. Xiao, Y. Peng, X. Wang, H. Li, F. Wei, Y. Lu, *Adv. Funct. Mater.* **2009**, 19, 3420.
- [11] C. K. Chan, H. Peng, G. Liu, K. McIlwrath, X. F. Zhang, R. A. Huggins, Y. Cui, *Nat. Nanotechnol.* **2008**, 3, 31.
- [12] V. Anh, Y. Qian, A. Stein, *Adv. Energy Mater.* **2012**, 2, 1056.
- [13] H. Zhang, X. Yu, P. V. Braun, *Nat. Nanotechnol.* **2011**, 6, 277.
- [14] Z.-S. Wu, Y. Sun, Y.-Z. Tan, S. Yang, X. Feng, K. Muellen, *J. Am. Chem. Soc.* **2012**, 134, 19532.
- [15] B. E. Conway, *J. Electrochem. Soc.* **1991**, 138, 1539.
- [16] C. Wu, X. Lu, L. Peng, K. Xu, X. Peng, J. Huang, G. Yu, Y. Xie, *Nat. Commun.* **2013**, 4, 2431.
- [17] D. Pech, M. Brunet, H. Durou, P. Huang, V. Mochalin, Y. Gogotsi, P.-L. Taberna, P. Simon, *Nat. Nanotechnol.* **2010**, 5, 651.
- [18] Y. Gogotsi, *Nature* **2014**, 509, 568.
- [19] L. Hu, H. Wu, F. La Mantia, Y. Yang, Y. Cui, *ACS Nano* **2010**, 4, 5843.
- [20] S. Xu, Y. Zhang, J. Cho, J. Lee, X. Huang, L. Jia, J. A. Fan, Y. Su, J. Su, H. Zhang, H. Cheng, B. Lu, C. Yu, C. Chuang, T.-i. Kim, T. Song, K. Shigeta, S. Kang, C. Dagdeviren, I. Petrov, P. V. Braun, Y. Huang, U. Paik, J. A. Rogers, *Nat. Commun.* **2013**, 4, 1543.
- [21] J. Ge, G. Cheng, L. Chen, *Nanoscale* **2011**, 3, 3084.
- [22] Y. Tian, S. Cong, W. Su, H. Chen, Q. Li, F. Geng, Z. Zhao, *Nano Lett.* **2014**, 14, 2150.
- [23] B. C. K. Tee, C. Wang, R. Allen, Z. Bao, *Nat. Nanotechnol.* **2012**, 7, 825.
- [24] Y. Dou, T. Pan, A. Zhou, S. Xu, X. Liu, J. Han, M. Wei, D. G. Evans, X. Duan, *Chem. Commun.* **2013**, 49, 8462.
- [25] S. W. Pan, H. J. Lin, J. Deng, P. N. Chen, X. L. Chen, Z. B. Yang, H. S. Peng, *Adv. Energy Mater.* **2015**, 5, 1401438.

- [26] K. Jost, C. R. Perez, J. K. McDonough, V. Presser, M. Heon, G. Dion, Y. Gogotsi, *Energy Environ. Sci.* **2011**, *4*, 5060.
- [27] W. Weng, Q. Sun, Y. Zhang, H. Lin, J. Ren, X. Lu, M. Wang, H. Peng, *Nano Lett.* **2014**, *14*, 3432.
- [28] P. Yang, W. Mai, *Nano Energy* **2014**, *8*, 274.
- [29] G. Zhou, F. Li, H.-M. Cheng, *Energy Environ. Sci.* **2014**, *7*, 1307.
- [30] L. Li, Z. Wu, S. Yuan, X.-B. Zhang, *Energy Environ. Sci.* **2014**, *7*, 2101.
- [31] X. Wang, X. Lu, B. Liu, D. Chen, Y. Tong, G. Shen, *Adv. Mater.* **2014**, *26*, 4763.
- [32] S. S. Zhang, *J. Power Sources* **2007**, *164*, 351.
- [33] J. Saunier, F. Alloin, J. Y. Sanchez, G. Caillon, *J. Power Sources* **2003**, *119*, 454.
- [34] J. Chen, *Materials* **2013**, *6*, 156.
- [35] A. S. Arico, P. Bruce, B. Scrosati, J. M. Tarascon, W. Van Schalkwijk, *Nat. Mater.* **2005**, *4*, 366.
- [36] M. Wakihara, *Mater. Sci. Eng. R-Rep* **2001**, *33*, 109.
- [37] H. Gwon, H.-S. Kim, K. U. Lee, D.-H. Seo, Y. C. Park, Y.-S. Lee, B. T. Ahn, K. Kang, *Energy Environ. Sci.* **2011**, *4*, 1277.
- [38] Y. Jiang, A. Kozinda, T. Chang, L. Lin, *Sensor Actuat A-Phys* **2013**, *195*, 224.
- [39] V. L. Pushparaj, M. M. Shaijumon, A. Kumar, S. Murugesan, L. Ci, R. Vajtai, R. J. Linhardt, O. Nalamasu, P. M. Ajayan, *Proc. Natl Acad. Sci. USA* **2007**, *104*, 13574.
- [40] D. P. Dubal, J. G. Kim, Y. Kim, R. Holze, C. D. Lokhande, W. B. Kim, *Energy Technol.* **2014**, *2*, 325.
- [41] Y.-Z. Zhang, Y. Wang, T. Cheng, W.-Y. Lai, H. Pang, W. Huang, *Chem. Soc. Rev.* **2015**, *44*, 5181.
- [42] S.-Y. Lee, K.-H. Choi, W.-S. Choi, Y. H. Kwon, H.-R. Jung, H.-C. Shin, J. Y. Kim, *Energy Environ. Sci.* **2013**, *6*, 2414.
- [43] X. Peng, L. Peng, C. Wu, Y. Xie, *Chem. Soc. Rev.* **2014**, *43*, 3303.
- [44] L. Nyholm, G. Nystrom, A. Mihranyan, M. Stromme, *Adv. Mater.* **2011**, *23*, 3751.
- [45] L. Shen, Q. Che, H. Li, X. Zhang, *Adv. Funct. Mater.* **2014**, *24*, 2630.
- [46] Q. Cheng, Z. Song, T. Ma, B. B. Smith, R. Tang, H. Yu, H. Jiang, C. K. Chan, *Nano Lett.* **2013**, *13*, 4969.
- [47] S.-L. Chou, J.-Z. Wang, S.-Y. Chew, H.-K. Liu, S.-X. Dou, *Electrochem. Commun.* **2008**, *10*, 1724.
- [48] L. Hu, W. Chen, X. Xie, N. Liu, Y. Yang, H. Wu, Y. Yao, M. Pasta, H. N. Alshareef, Y. Cui, *ACS Nano* **2011**, *5*, 8904.
- [49] W. Zhang, S. Yang, *Acc. Chem. Res.* **2009**, *42*, 1617.
- [50] J. M. Tarascon, M. Armand, *Nature* **2001**, *414*, 359.
- [51] A. Caballero, J. Morales, L. Sanchez, *Electrochem. Solid-State Lett.* **2005**, *8*, A464.
- [52] J. Li, R. Kloepsch, S. Nowak, M. Kunze, M. Winter, S. Passerini, *J. Power Sources* **2011**, *196*, 7687.
- [53] J. L. Gomez Camer, J. Morales, L. Sanchez, P. Ruch, S. H. Ng, R. Koetz, P. Novak, *Electrochim. Acta* **2009**, *54*, 6713.
- [54] N. Aliahmad, M. Agarwal, S. Shrestha, K. Varahramyan, *IEEE Trans. Nanotechnol.* **2013**, *12*, 408.
- [55] L. Hu, F. La Mantia, H. Wu, X. Xie, J. McDonough, M. Pasta, Y. Cui, *Adv. Energy Mater.* **2011**, *1*, 1012.
- [56] Y. Liu, S. Gorgutsa, C. Santato, M. Skorobogatiy, *J. Electrochem. Soc.* **2012**, *159*, A349.
- [57] Y.-H. Lee, J.-S. Kim, J. Noh, I. Lee, H. J. Kim, S. Choi, J. Seo, S. Jeon, T.-S. Kim, J.-Y. Lee, J. W. Choi, *Nano Lett.* **2013**, *13*, 5753.
- [58] C. Arbizzani, S. Beninati, M. Lazzari, M. Mastragostino, *J. Power Sources* **2005**, *141*, 149.
- [59] Q. Si, M. Matsui, T. Horiba, O. Yamamoto, Y. Takeda, N. Seki, N. Imanishi, *J. Power Sources* **2013**, *241*, 744.
- [60] C. Zhang, W. W. Tjiu, T. Liu, *Polym. Chem.* **2013**, *4*, 5785.
- [61] J. Zhang, X. Wang, J. Ma, S. Liu, X. Yi, *Electrochim. Acta* **2013**, *104*, 110.
- [62] L.-F. Cui, L. Hu, J. W. Choi, Y. Cui, *ACS Nano* **2010**, *4*, 3671.
- [63] B. J. Landi, M. J. Ganter, C. D. Cress, R. A. DiLeo, R. P. Raffaele, *Energy Environ. Sci.* **2009**, *2*, 638.
- [64] S. H. Ng, J. Wang, Z. P. Guo, G. X. Wang, H. K. Liu, *Electrochim. Acta* **2005**, *51*, 23.
- [65] X. Huang, Z. Yin, S. Wu, X. Qi, Q. He, Q. Zhang, Q. Yan, F. Boey, H. Zhang, *Small* **2011**, *7*, 1876.
- [66] D. Chen, L. Tang, J. Li, *Chem. Soc. Rev.* **2010**, *39*, 3157.
- [67] V. Singh, D. Joung, L. Zhai, S. Das, S. I. Khondaker, S. Seal, *Prog. Mater. Sci.* **2011**, *56*, 1178.
- [68] H.-X. Zhang, C. Feng, Y.-C. Zhai, K.-L. Jiang, Q.-Q. Li, S.-S. Fan, *Adv. Mater.* **2009**, *21*, 2299.
- [69] J. K. Lee, K. B. Smith, C. M. Hayner, H. H. Kung, *Chem. Commun.* **2010**, *46*, 2025.
- [70] Y. Hu, X. Li, J. Wang, R. Li, X. Sun, *J. Power Sources* **2013**, *237*, 41.
- [71] S. Y. Chew, S. H. Ng, J. Wang, P. Novak, F. Krumeich, S. L. Chou, J. Chen, H. K. Liu, *Carbon* **2009**, *47*, 2976.
- [72] C. Zhong, J.-Z. Wang, D. Wexler, H.-K. Liu, *Carbon* **2014**, *66*, 637.
- [73] J. Ren, L. Li, C. Chen, X. Chen, Z. Cai, L. Qiu, Y. Wang, X. Zhu, H. Peng, *Adv. Mater.* **2013**, *25*, 1155.
- [74] L. Noerchim, J.-Z. Wang, S.-L. Chou, D. Wexler, H.-K. Liu, *Carbon* **2012**, *50*, 1289.
- [75] R. Chen, T. Zhao, W. Wu, F. Wu, L. Li, J. Qian, R. Xu, H. Wu, H. M. Albishri, A. S. Al-Bogami, D. Abd El-Hady, J. Lu, K. Amine, *Nano Lett.* **2014**, *14*, 5899.
- [76] T. Gao, K. Huang, X. Qi, H. Li, L. Yang, J. Zhong, *Ceram. Int.* **2014**, *40*, 6891.
- [77] B. Wang, X. Li, B. Luo, Y. Jia, L. Zhi, *Nanoscale* **2013**, *5*, 1470.
- [78] Z. Song, T. Ma, R. Tang, Q. Cheng, X. Wang, D. Krishnaraju, R. Panat, C. K. Chan, H. Yu, H. Jiang, *Nat. Commun.* **2014**, *5*, 3140.
- [79] Y. H. Kwon, S.-W. Woo, H.-R. Jung, H. K. Yu, K. Kim, B. H. Oh, S. Ahn, S.-Y. Lee, S.-W. Song, J. Cho, H.-C. Shin, J. Y. Kim, *Adv. Mater.* **2012**, *24*, 5192.
- [80] H. Lin, W. Weng, J. Ren, L. Qiu, Z. Zhang, P. Chen, X. Chen, J. Deng, Y. Wang, H. Peng, *Adv. Mater.* **2014**, *26*, 1217.
- [81] M. Park, D. S. Shin, J. Ryu, M. Choi, N. Park, S. Y. Hong, J. Cho, *Adv. Mater.* **2015**, *27*, 5141.
- [82] J. F. Ihlefeld, P. G. Clem, B. L. Doyle, P. G. Kotula, K. R. Fenton, C. A. Apple, *Adv. Mater.* **2011**, *23*, 5663.
- [83] S.-H. Kim, K.-H. Choi, S.-J. Cho, J.-S. Park, K. Y. Cho, C. K. Lee, S. B. Lee, J. K. Shim, S.-Y. Lee, *J. Mater. Chem. A* **2014**, *2*, 10854.
- [84] X. Ma, X. Huang, J. Gao, S. Zhang, Z. Peng, Z. Deng, J. Suo, *J. Power Sources* **2014**, *272*, 259.
- [85] K.-H. Choi, S.-J. Cho, S.-H. Kim, Y. H. Kwon, J. Y. Kim, S.-Y. Lee, *Adv. Funct. Mater.* **2014**, *24*, 44.
- [86] G. Hirankumar, S. Selvasekarapandian, N. Kuwata, J. Kawamura, T. Hattori, *J. Power Sources* **2005**, *144*, 262.
- [87] Z. Niu, L. Zhang, L. Liu, B. Zhu, H. Dong, X. Chen, *Adv. Mater.* **2013**, *25*, 4035.
- [88] G. Wang, X. Lu, Y. Ling, T. Zhai, H. Wang, Y. Tong, Y. Li, *ACS Nano* **2012**, *6*, 10296.
- [89] X. Lu, M. Yu, G. Wang, Y. Tong, Y. Li, *Energy Environ. Sci.* **2014**, *7*, 2160.
- [90] N. A. Choudhury, S. Sampath, A. K. Shukla, *Energy Environ. Sci.* **2009**, *2*, 55.
- [91] K. V. Sankar, R. K. Selvan, *Carbon* **2015**, *90*, 260.
- [92] A. A. Latoszynska, G. Z. Zukowska, I. A. Rutkowska, P.-L. Taberna, P. Simon, P. J. Kulesza, W. Wieczorek, *J. Power Sources* **2015**, *274*, 1147.
- [93] M. Egashira, Y. Matsuno, N. Yoshimoto, M. Morita, *J. Power Sources* **2010**, *195*, 3036.
- [94] C. Zhou, Y. Zhang, Y. Li, J. Liu, *Nano Lett.* **2013**, *13*, 2078.
- [95] G. A. Snook, P. Kao, A. S. Best, *J. Power Sources* **2011**, *196*, 1.
- [96] J. Zhang, X. S. Zhao, *J. Phys. Chem. C* **2012**, *116*, 5420.
- [97] H. Gomez, M. K. Ram, F. Alvi, P. Villalba, E. Stefanakos, A. Kumar, *J. Power Sources* **2011**, *196*, 4102.
- [98] H.-P. Cong, X.-C. Ren, P. Wang, S.-H. Yu, *Energy Environ. Sci.* **2013**, *6*, 1185.



- [99] B. Yao, L. Yuan, X. Xiao, J. Zhang, Y. Qi, J. Zhou, J. Zhou, B. Hu, W. Chen, *Nano Energy* **2013**, *2*, 1071.
- [100] C. Yan, P. S. Lee, *Small* **2014**, *10*, 3443.
- [101] K. Xie, B. Wei, *Adv. Mater.* **2014**, *26*, 3592.
- [102] T. Chen, H. Peng, M. Durstock, L. Dai, *Sci. Rep.* **2014**, *4*, 3612.
- [103] Q. Cao, S. H. Hur, Z. T. Zhu, Y. G. Sun, C. J. Wang, M. A. Meitl, M. Shim, J. A. Rogers, *Adv. Mater.* **2006**, *18*, 304.
- [104] D. J. Lipomi, M. Vosgueritchian, B. C. K. Tee, S. L. Hellstrom, J. A. Lee, C. H. Fox, Z. Bao, *Nat. Nanotechnol.* **2011**, *6*, 788.
- [105] H. Lee, J.-K. Yoo, J.-H. Park, J. H. Kim, K. Kang, Y. S. Jung, *Adv. Energy Mater.* **2012**, *2*, 976.
- [106] K.-Y. Chun, Y. Oh, J. Rho, J.-H. Ahn, Y.-J. Kim, H. R. Choi, S. Baik, *Nat. Nanotechnol.* **2010**, *5*, 853.
- [107] F. Li, J. Chen, X. Wang, M. Xue, G. F. Chen, *Adv. Funct. Mater.* **2015**, *25*, 4601.
- [108] N. Li, G. Yang, Y. Sun, H. Song, H. Cui, G. Yang, C. Wang, *Nano Lett.* **2015**, *15*, 3195.
- [109] C. Yu, C. Masarapu, J. Rong, B. Wei, H. Jiang, *Adv. Mater.* **2009**, *21*, 4793.
- [110] T. Chen, Y. Xue, A. K. Roy, L. Dai, *ACS Nano* **2014**, *8*, 1039.
- [111] Z. Niu, H. Dong, B. Zhu, J. Li, H. H. Hng, W. Zhou, X. Chen, S. Xie, *Adv. Mater.* **2013**, *25*, 1058.
- [112] D. J. Lipomi, B. C. K. Tee, M. Vosgueritchian, Z. Bao, *Adv. Mater.* **2011**, *23*, 1771.
- [113] Y. Sun, W. M. Choi, H. Jiang, Y. Y. Huang, J. A. Rogers, *Nat. Nanotechnol.* **2006**, *1*, 201.
- [114] W. Weng, Q. Sun, Y. Zhang, S. He, Q. Wu, J. Deng, X. Fang, G. Guan, J. Ren, H. Peng, *Adv. Mater.* **2015**, *27*, 1363.
- [115] D. Kim, G. Shin, Y. J. Kang, W. Kim, J. S. Ha, *ACS Nano* **2013**, *7*, 7975.
- [116] Z. Song, X. Wang, C. Lv, Y. An, M. Liang, T. Ma, D. He, Y.-J. Zheng, S.-Q. Huang, H. Yu, H. Jiang, *Sci. Rep.* **2015**, *5*, 10988.
- [117] S. P. Lacour, J. Jones, S. Wagner, T. Li, Z. G. Suo, *Proc. IEEE* **2005**, *93*, 1459.
- [118] B. Yue, C. Wang, X. Ding, G. G. Wallace, *Electrochim. Acta* **2012**, *68*, 18.
- [119] M. J. Yun, S. I. Cha, S. H. Seo, D. Y. Lee, *Sci. Rep.* **2014**, *4*, 5322.
- [120] K. Xie, J. Li, Y. Lai, Z. a. Zhang, Y. Liu, G. Zhang, H. Huang, *Nanoscale* **2011**, *3*, 2202.
- [121] L. Hu, M. Pasta, F. La Mantia, L. Cui, S. Jeong, H. D. Deshazer, J. W. Choi, S. M. Han, Y. Cui, *Nano Lett.* **2010**, *10*, 708.
- [122] K. Jost, D. Stenger, C. R. Perez, J. K. McDonough, K. Lian, Y. Gogotsi, G. Dion, *Energy Environ. Sci.* **2013**, *6*, 2698.
- [123] T. G. Yun, M. Oh, L. Hu, S. Hyun, S. M. Han, *J. Power Sources* **2013**, *244*, 783.
- [124] P. Xu, B. Wei, Z. Cao, J. Zheng, K. Gong, F. Li, J. Yu, Q. Li, W. Lu, J.-H. Byun, B.-S. Kim, Y. Yan, T.-W. Chou, *ACS Nano* **2015**, *9*, 6088.
- [125] Y. Meng, Y. Zhao, C. Hu, H. Cheng, Y. Hu, Z. Zhang, G. Shi, L. Qu, *Adv. Mater.* **2013**, *25*, 2326.
- [126] Y. Zhang, W. Bai, J. Ren, W. Weng, H. Lin, Z. Zhang, H. Peng, *J. Mater. Chem. A* **2014**, *2*, 11054.
- [127] Y. Shang, X. He, Y. Li, L. Zhang, Z. Li, C. Ji, E. Shi, P. Li, K. Zhu, Q. Peng, C. Wang, X. Zhang, R. Wang, J. Wei, K. Wang, H. Zhu, D. Wu, A. Cao, *Adv. Mater.* **2012**, *24*, 2896.
- [128] C. Choi, S. H. Kim, H. J. Sim, J. A. Lee, A. Y. Choi, Y. T. Kim, X. Lepro, G. M. Spinks, R. H. Baughman, S. J. Kim, *Sci. Rep.* **2015**, *5*, 9387.
- [129] Y. Zhang, W. Bai, X. Cheng, J. Ren, W. Weng, P. Chen, X. Fang, Z. Zhang, H. Peng, *Angew. Chem. Int. Ed.* **2014**, *53*, 14564.
- [130] Z. Yang, J. Deng, X. Chen, J. Ren, H. Peng, *Angew. Chem. Int. Ed.* **2013**, *52*, 13453.
- [131] B. A. Taleatu, E. A. A. Arbab, E. Omotoso, G. T. Mola, *J. Microsc.* **2014**, *256*, 61.
- [132] K. Wang, H. Wu, Y. Meng, Y. Zhang, Z. Wei, *Energy Environ. Sci.* **2012**, *5*, 8384.
- [133] P.-C. Chen, G. Shen, S. Sukcharoenchoke, C. Zhou, *Appl. Phys. Lett.* **2009**, *94*, 043113.
- [134] X. Wang, K. Gao, Z. Shao, X. Peng, X. Wu, F. Wang, *J. Power Sources* **2014**, *249*, 148.
- [135] H. Chen, S. Zeng, M. Chen, Y. Zhang, Q. Li, *Carbon* **2015**, *92*, 271.
- [136] K. Devarayan, D. Lei, H.-Y. Kim, B.-S. Kim, *Chem. Eng. J.* **2015**, *273*, 603.
- [137] K. Gao, Z. Shao, X. Wu, X. Wang, Y. Zhang, W. Wang, F. Wang, *Nanoscale* **2013**, *5*, 5307.
- [138] J. Wan, W. Bao, Y. Liu, J. Dai, F. Shen, L. Zhou, X. Cai, D. Urban, Y. Li, K. Jungjohann, M. S. Fuhrer, L. Hu, *Adv. Energy Mater.* **2015**, *5*, 1401742.
- [139] T. Qiu, B. Luo, M. Giersig, E. M. Akinoglu, L. Hao, X. Wang, L. Shi, M. Jin, L. Zhi, *Small* **2014**, *10*, 4136.
- [140] I. Ryu, M. Yang, H. Kwon, H. K. Park, Y. R. Do, S. B. Lee, S. Yim, *Langmuir* **2014**, *30*, 1704.
- [141] F. Mirri, A. W. K. Ma, T. T. Hsu, N. Behabtu, S. L. Eichmann, C. C. Young, D. E. Tsentelovich, M. Pasquali, *ACS Nano* **2012**, *6*, 9737.
- [142] V. C. Tung, L.-M. Chen, M. J. Allen, J. K. Wassei, K. Nelson, R. B. Kaner, Y. Yang, *Nano Lett.* **2009**, *9*, 1949.
- [143] P. Xu, J. Kang, J.-B. Choi, J. Suhr, J. Yu, F. Li, J.-H. Byun, B.-S. Kim, T.-W. Chou, *ACS Nano* **2014**, *8*, 9437.
- [144] D. Wei, M. R. J. Scherer, C. Bower, P. Andrew, T. Ryhaenen, U. Steiner, *Nano Lett.* **2012**, *12*, 1857.
- [145] X. Chen, H. Lin, P. Chen, G. Guan, J. Deng, H. Peng, *Adv. Mater.* **2014**, *26*, 4444.
- [146] X. Chen, H. Lin, J. Deng, Y. Zhang, X. Sun, P. Chen, X. Fang, Z. Zhang, G. Guan, H. Peng, *Adv. Mater.* **2014**, *26*, 8126.
- [147] A. M. Oesterholm, D. E. Shen, A. L. Dyer, J. R. Reynolds, *ACS Appl. Mater. Interfaces* **2013**, *5*, 13432.
- [148] L. Liu, J. Zhao, P. J. Culligan, Y. Qiao, X. Chen, *Langmuir* **2009**, *25*, 11862.
- [149] J. Shen, K. Han, E. J. Martin, Y. Y. Wu, M. C. Kung, C. M. Hayner, K. R. Shull, H. H. Kung, *J. Mater. Chem. A* **2014**, *2*, 18204.
- [150] Y. Huang, Y. Huang, M. Zhu, W. Meng, Z. Pei, C. Liu, H. Hu, C. Zhi, *ACS Nano* **2015**, *9*, 6242.
- [151] X. Liu, D. Wu, H. Wang, Q. Wang, *Adv. Mater.* **2014**, *26*, 4370.
- [152] C. Wang, H. Wu, Z. Chen, M. T. McDowell, Y. Cui, Z. Bao, *Nat. Chem.* **2013**, *5*, 1042.
- [153] H. Wang, B. Zhu, W. Jiang, Y. Yang, W. R. Leow, H. Wang, X. Chen, *Adv. Mater.* **2014**, *26*, 3638.
- [154] Y. Zhu, C. Yao, J. Ren, C. Liu, L. Ge, *Colloid. Surface. A.* **2015**, *465*, 26.
- [155] H. Sun, X. You, Y. Jiang, G. Guan, X. Fang, J. Deng, P. Chen, Y. Luo, H. Peng, *Angew. Chem. Int. Ed.* **2014**, *53*, 9526.
- [156] J. R. Miller, R. A. Outlaw, B. C. Holloway, *Science* **2010**, *329*, 1637.
- [157] Z.-S. Wu, Z. Liu, K. Parvez, X. Feng, K. Muellen, *Adv. Mater.* **2015**, *27*, 3669.
- [158] B. Oregan, M. Gratzel, *Nature* **1991**, *353*, 737.
- [159] M. Gratzel, *Inorg. Chem.* **2005**, *44*, 6841.
- [160] Z. Yin, J. Zhu, Q. He, X. Cao, C. Tan, H. Chen, Q. Yan, H. Zhang, *Adv. Energy Mater.* **2014**, *4*, 1300594.
- [161] Y.-G. Guo, J.-S. Hu, L.-J. Wan, *Adv. Mater.* **2008**, *20*, 2878.
- [162] J. Jiang, Y. Li, J. Liu, X. Huang, C. Yuan, X. W. Lou, *Adv. Mater.* **2012**, *24*, 5166.
- [163] G. J. Snyder, E. S. Toberer, *Nat. Mater.* **2008**, *7*, 105.
- [164] B. Poudel, Q. Hao, Y. Ma, Y. Lan, A. Minnich, B. Yu, X. Yan, D. Wang, A. Muto, D. Vashaee, X. Chen, J. Liu, M. S. Dresselhaus, G. Chen, Z. Ren, *Science* **2008**, *320*, 634.
- [165] W. Liu, X. Yan, G. Chen, Z. Ren, *Nano Energy* **2012**, *1*, 42.
- [166] A. Hagfeldt, G. Boschloo, L. Sun, L. Kloo, H. Pettersson, *Chem. Rev.* **2010**, *110*, 6595.
- [167] B. Tian, X. Zheng, T. J. Kempa, Y. Fang, N. Yu, G. Yu, J. Huang, C. M. Lieber, *Nature* **2007**, *449*, 885.

- [168] Z. L. Wang, J. H. Song, *Science* **2006**, 312, 242.
- [169] X. Wang, *Nano Energy* **2012**, 1, 13.
- [170] Z. L. Wang, G. Zhu, Y. Yang, S. Wang, C. Pan, *Mater. Today* **2012**, 15, 532.
- [171] S. N. Cha, J.-S. Seo, S. M. Kim, H. J. Kim, Y. J. Park, S.-W. Kim, J. M. Kim, *Adv. Mater.* **2010**, 22, 4726.
- [172] G. Zhu, Z.-H. Lin, Q. Jing, P. Bai, C. Pan, Y. Yang, Y. Zhou, Z. L. Wang, *Nano Lett.* **2013**, 13, 847.
- [173] R. G. Horn, D. T. Smith, *Science* **1992**, 256, 362.
- [174] R. G. Horn, D. T. Smith, A. Grabbe, *Nature* **1993**, 366, 442.
- [175] S. Niu, Y. Liu, S. Wang, L. Lin, Y. S. Zhou, Y. Hu, Z. L. Wang, *Adv. Mater.* **2013**, 25, 6184.
- [176] X. Pu, L. Li, H. Song, C. Du, Z. Zhao, C. Jiang, G. Cao, W. Hu, Z. L. Wang, *Adv. Mater.* **2015**, 27, 2472.
- [177] X. Xue, S. Wang, W. Guo, Y. Zhang, Z. L. Wang, *Nano Lett.* **2012**, 12, 5048.
- [178] X. Xue, P. Deng, B. He, Y. Nie, L. Xing, Y. Zhang, Z. L. Wang, *Adv. Energy Mater.* **2014**, 4, 1301329.
- [179] L. Xing, Y. Nie, X. Xue, Y. Zhang, *Nano Energy* **2014**, 10, 44.
- [180] X. Xue, P. Deng, S. Yuan, Y. Nie, B. He, L. Xing, Y. Zhang, *Energy Environ. Sci.* **2013**, 6, 2615.
- [181] A. S. Westover, K. Share, R. Carter, A. P. Cohn, L. Oakes, C. L. Pint, *Appl. Phys. Lett.* **2014**, 104, 213905.
- [182] C.-T. Chien, P. Hiralal, D.-Y. Wang, I. S. Huang, C.-C. Chen, C.-W. Chen, G. A. J. Amaratunga, *Small* **2015**, 11, 2929.
- [183] C.-Y. Hsu, H.-W. Chen, K.-M. Lee, C.-W. Hu, K.-C. Ho, *J. Power Sources* **2010**, 195, 6232.
- [184] A. Hauch, A. Georg, U. O. Krasovec, B. Orel, *J. Electrochem. Soc.* **2002**, 149, A1208.
- [185] H.-W. Chen, C.-Y. Hsu, J.-G. Chen, K.-M. Lee, C.-C. Wang, K.-C. Huang, K.-C. Ho, *J. Power Sources* **2010**, 195, 6225.
- [186] G. Wee, T. Salim, Y. M. Lam, S. G. Mhaisalkar, M. Srinivasan, *Energy Environ. Sci.* **2011**, 4, 413.
- [187] T. Miyasaka, T. N. Murakami, *Appl. Phys. Lett.* **2004**, 85, 3932.
- [188] T. N. Murakami, N. Kawashima, T. Miyasaka, *Chem. Commun.* **2005**, 41, 3346.
- [189] W. J. Lee, E. Ramasamy, D. Y. Lee, J. S. Song, *ACS Appl. Mater. Interfaces* **2009**, 1, 1145.
- [190] L. Hu, D. S. Hecht, G. Gruener, *Chem. Rev.* **2010**, 110, 5790.
- [191] P. Simon, Y. Gogotsi, *Acc. Chem. Res.* **2013**, 46, 1094.
- [192] L. L. Zhang, X. S. Zhao, *Chem. Soc. Rev.* **2009**, 38, 2520.
- [193] L. Hu, J. W. Choi, Y. Yang, S. Jeong, F. La Mantia, L.-F. Cui, Y. Cui, *Proc. Natl Acad. Sci. USA* **2009**, 106, 21490.
- [194] K. H. An, W. S. Kim, Y. S. Park, Y. C. Choi, S. M. Lee, D. C. Chung, D. J. Bae, S. C. Lim, Y. H. Lee, *Adv. Mater.* **2001**, 13, 497.
- [195] Z. Yang, L. Li, Y. Luo, R. He, L. Qiu, H. Lin, H. Peng, *J. Mater. Chem. A* **2013**, 1, 954.
- [196] J. Xu, H. Wu, L. Lu, S.-F. Leung, D. Chen, X. Chen, Z. Fan, G. Shen, D. Li, *Adv. Funct. Mater.* **2014**, 24, 1840.
- [197] W. Guo, X. Xue, S. Wang, C. Lin, Z. L. Wang, *Nano Lett.* **2012**, 12, 2520.
- [198] M. Skunik-Nuckowska, K. Grzejszczyk, P. J. Kulesza, L. Yang, N. Vlachopoulos, L. Haggman, E. Johansson, A. Hagfeldt, *J. Power Sources* **2013**, 234, 91.
- [199] X. Fan, Z. Chu, F. Wang, C. Zhang, L. Chen, Y. Tang, D. Zou, *Adv. Mater.* **2008**, 20, 592.
- [200] D. Zou, D. Wang, Z. Chu, Z. Lv, X. Fan, *Coord. Chem. Rev.* **2010**, 254, 1169.
- [201] T. Chen, L. Qiu, Z. Cai, F. Gong, Z. Yang, Z. Wang, H. Peng, *Nano Lett.* **2012**, 12, 2568.
- [202] S. Pan, Z. Yang, H. Li, L. Qiu, H. Sun, H. Peng, *J. Am. Chem. Soc.* **2013**, 135, 10622.
- [203] Z. Yang, H. Sun, T. Chen, L. Qiu, Y. Luo, H. Peng, *Angew. Chem. Int. Ed.* **2013**, 52, 7545.
- [204] S. Pan, Z. Yang, P. Chen, X. Fang, G. Guan, Z. Zhang, J. Deng, H. Peng, *J. Phys. Chem. C* **2014**, 118, 16419.
- [205] H. Sun, X. You, J. Deng, X. Chen, Z. Yang, P. Chen, X. Fang, H. Peng, *Angew. Chem. Int. Ed.* **2014**, 53, 6664.
- [206] S. Pan, Z. Zhang, W. Weng, H. Lin, Z. Yang, H. Peng, *Mater. Today* **2014**, 17, 276.
- [207] Y. Fu, X. Cai, H. Wu, Z. Lv, S. Hou, M. Peng, X. Yu, D. Zou, *Adv. Mater.* **2012**, 24, 5713.
- [208] B. Liu, D. Tan, X. Wang, D. Chen, G. Shen, *Small* **2013**, 9, 1998.
- [209] X. Wang, B. Liu, R. Liu, Q. Wang, X. Hou, D. Chen, R. Wang, G. Shen, *Angew. Chem. Int. Ed.* **2014**, 53, 1849.
- [210] Q. Meng, H. Wu, Y. Meng, K. Xie, Z. Wei, Z. Guo, *Adv. Mater.* **2014**, 26, 4100.
- [211] K. Wang, Q. Meng, Y. Zhang, Z. Wei, M. Miao, *Adv. Mater.* **2013**, 25, 1494.
- [212] X. Li, X. Zang, Z. Li, X. Li, P. Li, P. Sun, X. Lee, R. Zhang, Z. Huang, K. Wang, D. Wu, F. Kang, H. Zhu, *Adv. Funct. Mater.* **2013**, 23, 4862.
- [213] J. A. Lee, M. K. Shin, S. H. Kim, H. U. Cho, G. M. Spinks, G. G. Wallace, M. D. Lima, X. Lepro, M. E. Kozlov, R. H. Baughman, S. J. Kim, *Nat. Commun.* **2013**, 4, 1970.
- [214] N. Liu, W. Ma, J. Tao, X. Zhang, J. Su, L. Li, C. Yang, Y. Gao, D. Golberg, Y. Bando, *Adv. Mater.* **2013**, 25, 4925.
- [215] D. Yu, K. Goh, H. Wang, L. Wei, W. Jiang, Q. Zhang, L. Dai, Y. Chen, *Nat. Nanotechnol.* **2014**, 9, 555.
- [216] L. Kou, T. Huang, B. Zheng, Y. Han, X. Zhao, K. Gopalsamy, H. Sun, C. Gao, *Nat. Commun.* **2014**, 5, 3754.
- [217] G. Sun, X. Zhang, R. Lin, J. Yang, H. Zhang, P. Chen, *Angew. Chem. Int. Ed.* **2015**, 54, 4651.
- [218] S. Pan, J. Deng, G. Guan, Y. Zhang, P. Chen, J. Ren, H. Peng, *J. Mater. Chem. A* **2015**, 3, 6286.
- [219] L. Liu, Y. Yu, C. Yan, K. Li, Z. Zheng, *Nat. Commun.* **2015**, 6, 7260.
- [220] T. Chen, L. Qiu, Z. Yang, Z. Cai, J. Ren, H. Li, H. Lin, X. Sun, H. Peng, *Angew. Chem. Int. Ed.* **2012**, 51, 11977.
- [221] Y. Fu, H. Wu, S. Ye, X. Cai, X. Yu, S. Hou, H. Kafay, D. Zou, *Energy Environ. Sci.* **2013**, 6, 805.
- [222] Z. Zhang, X. Chen, P. Chen, G. Guan, L. Qiu, H. Lin, Z. Yang, W. Bai, Y. Luo, H. Peng, *Adv. Mater.* **2014**, 26, 466.
- [223] X. Chen, H. Sun, Z. Yang, G. Guan, Z. Zhang, L. Qiu, H. Peng, *J. Mater. Chem. A* **2014**, 2, 1897.
- [224] Z. Yang, J. Deng, H. Sun, J. Ren, S. Pan, H. Peng, *Adv. Mater.* **2014**, 26, 7038.
- [225] H. Sun, H. Li, X. You, Z. Yang, J. Deng, L. Qiu, H. Peng, *J. Mater. Chem. A* **2014**, 2, 345.
- [226] X. Chen, L. Qiu, J. Ren, G. Guan, H. Lin, Z. Zhang, P. Chen, Y. Wang, H. Peng, *Adv. Mater.* **2013**, 25, 6436.
- [227] L. Viet Thong, H. Kim, A. Ghosh, J. Kim, J. Chang, V. Quoc An, P. Duy Tho, J.-H. Lee, S.-W. Kim, Y. H. Lee, *ACS Nano* **2013**, 7, 5940.
- [228] J. Burschka, N. Pellet, S.-J. Moon, R. Humphry-Baker, P. Gao, M. K. Nazeeruddin, M. Graetzel, *Nature* **2013**, 499, 316.
- [229] J. M. Ball, M. M. Lee, A. Hey, H. J. Snaith, *Energy Environ. Sci.* **2013**, 6, 1739.
- [230] P. Docampo, F. C. Hanusch, S. D. Stranks, M. Doeblinger, J. M. Feckl, M. Ehrensperger, N. K. Minar, M. B. Johnston, H. J. Snaith, T. Bein, *Adv. Energy Mater.* **2014**, 4, 1400355.
- [231] B. Conings, L. Baeten, C. De Dobbelaere, J. D'Haen, J. Manca, H.-G. Boyen, *Adv. Mater.* **2014**, 26, 2041.
- [232] N. Ahn, D.-Y. Son, I.-H. Jang, S. M. Kang, M. Choi, N.-G. Park, *J. Am. Chem. Soc.* **2015**, 137, 8696.
- [233] X. Li, M. I. Dar, C. Yi, J. Luo, M. Tschumi, S. M. Zakeeruddin, M. K. Nazeeruddin, H. Han, M. Graetzel, *Nat. Chem.* **2015**, 7, 703.
- [234] W. Nie, H. Tsai, R. Asadpour, J.-C. Blancon, A. J. Neukirch, G. Gupta, J. J. Crochet, M. Chhowalla, S. Tretiak, M. A. Alam, H.-L. Wang, A. D. Mohite, *Science* **2015**, 347, 522.
- [235] H. Zhou, Q. Chen, G. Li, S. Luo, T.-b. Song, H.-S. Duan, Z. Hong, J. You, Y. Liu, Y. Yang, *Science* **2014**, 345, 542.

- [236] L. Qiu, J. Deng, X. Lu, Z. Yang, H. Peng, *Angew. Chem. Int. Ed.* **2014**, *53*, 10425.
- [237] Z. Yang, J. Deng, X. Sun, H. Li, H. Peng, *Adv. Mater.* **2014**, *26*, 2643.
- [238] K. Wang, P. Zhao, X. Zhou, H. Wu, Z. Wei, *J. Mater. Chem.* **2011**, *21*, 16373.
- [239] W.-w. Liu, X.-b. Yan, J.-w. Lang, C. Peng, Q.-j. Xue, *J. Mater. Chem.* **2012**, *22*, 17245.
- [240] M. Pasta, F. La Mantia, L. Hu, H. D. Deshazer, Y. Cui, *Nano Res.* **2010**, *3*, 452.
- [241] G. Wang, H. Wang, X. Lu, Y. Ling, M. Yu, T. Zhai, Y. Tong, Y. Li, *Adv. Mater.* **2014**, *26*, 2676.
- [242] L. Bao, X. Li, *Adv. Mater.* **2012**, *24*, 3246.
- [243] K. Jost, D. P. Durkin, L. M. Haverhals, E. K. Brown, M. Langenstein, H. C. De Long, P. C. Trulove, Y. Gogotsi, G. Dion, *Adv. Energy Mater.* **2015**, *5*, 1401286.
- [244] A. B. Dalton, S. Collins, E. Munoz, J. M. Razal, V. H. Ebron, J. P. Ferraris, J. N. Coleman, B. G. Kim, R. H. Baughman, *Nature* **2003**, *423*, 703.